

This is the **accepted version** of the journal article:

Ugone, Valeria; Sanna, Daniele; Sciortino, Giuseppe; [et al.]. «Interaction of Vanadium(IV) Species with Ubiquitin : A Combined Instrumental and Computational Approach». *Inorganic Chemistry*, Vol. 58, Issue 12 (June 2019), p. 8064-8078. DOI 10.1021/acs.inorgchem.9b00807

This version is available at <https://ddd.uab.cat/record/281970>

under the terms of the  **CC BY-NC-ND** license

Interaction of Vanadium(IV) Species with Ubiquitin: a Combined Instrumental and Computational Approach

Valeria Ugone,[§] Daniele Sanna,^{†} Giuseppe Sciortino,^{§,#} Jean-Didier Maréchal,[#] and Eugenio Garribba^{*.§}*

[§] Dipartimento di Chimica e Farmacia, Università di Sassari, Via Vienna 2, I-07100 Sassari, Italy

[†] Istituto di Chimica Biomolecolare, Consiglio Nazionale delle Ricerche, Trav. La Crucca 3, I-07040 Sassari, Italy

[#] Departament de Química, Universitat Autònoma de Barcelona, 08193 Cerdanyola del Vallés, Barcelona, Spain

Corresponding authors. E-mail: daniele.sanna@cnr.it (D.S.); garrimba@uniss.it (E.G.).

Abstract

The interaction of $V^{IV}O^{2+}$ ion and five $V^{IV}OL_2$ compounds with potential pharmacological application, where L indicates maltolate (ma), kojate (koj), acetylacetonate (acac), 1,2-dimethyl-3-hydroxy-4(1*H*)-pyridinonate (dhp) and L-mimosinate (mim), with ubiquitin (Ub) was studied by EPR, ESI-MS, and computational (docking and DFT) methods. The free metal ion $V^{IV}O^{2+}$ interacts with Glu, Asp, His, Thr and Leu residues, but the most stable sites (named **1** and **2**) involve the coordination of (Glu16, Glu18) and (Glu24, Asp52). In the system with $V^{IV}OL_2$ compounds, the type of binding depends on the vanadium concentration. When the V concentration is in the mM range, the interaction occurs with *cis*- $VOL_2(H_2O)$, L = ma, koj, dhp and mim, or with $VO(acac)_2$: in the first case the equatorial coordination of His68, Glu16, Glu18 or Asp21 residues yields species with formula $n[VOL_2]-Ub$ where $n = 2-3$, while with $VO(acac)_2$ only non-covalent surface interactions are revealed. When the concentration of V is in the order of μM , the mono-chelated species $VOL(H_2O)_2^+$ with L = ma, koj, acac, dhp and mim, favored by the hydrolysis, interact with Ub, and adducts with composition $n[VOL]-Ub$ ($n = 1-2$) are observed with the contemporaneous coordination of (Glu18, Asp21) or (Glu16, Glu18) and (Glu24, Asp52) or (Glu51, Asp52) donors. The results of this work suggest that the combined application of spectroscopic, spectrometric and computational techniques allow the complete characterization of the ternary systems formed by a V compound and a model protein such as ubiquitin. The same approach can be applied, eventually changing the spectroscopic/spectrometric techniques, to study the interaction of other metal species with other proteins.

Introduction

One of the most interesting and promising application of the vanadium chemistry is the development of V based potential drugs.^{1, 2, 3, 4, 5} The interaction of V inorganic and complexed species with proteins is essential to explain their biological and pharmacological effects in the organism.⁶ The binding to blood serum proteins, such as transferrin (hTf) and albumin (HSA), influences the transport toward the target organs,^{6-7, 8, 9, 10, 11} and the uptake into cells. In fact, V can bind to the active sites of transferrin left free by Fe^{3+} (ca. 40% which corresponds to a concentration of 25 μM of free sites) and form mixed V–L–apo/holo-hTf species, which can be recognized by the cellular receptors in the endocytosis. Moreover, the binding to the cellular components can determine the pharmacological action or stabilize specific species in the cytosol: for example, $\text{H}_2\text{V}^{\text{V}}\text{O}_4^-$, because of the similarity with phosphate, inhibits the phosphatase enzymes accounting for the antidiabetic activity of V compounds,^{12, 13} and the potential antitumor, antiviral and antibacterial decavanadate(V)¹⁴ is stabilized after the interaction with ferritin and actin.¹⁵

Based on these premises, the study of the systems formed by V compounds with proteins appears to be fundamental to increase the knowledge of the type of binding, the number of the species interacting, and the region of the proteins where the binding occurs. The characterization of such systems is complicated by the possibility of two kinds of interaction: a passive binding on the protein surface involving only secondary interactions and an active binding with the formation of one or more coordination bonds.¹⁶

The structure, activity and function of V–proteins have been discussed from many years. After the pioneering works of Chasteen,¹⁷ several reviews have been published and the interested readers are referred to such studies.^{6, 18} Most of X-ray determinations for these systems concern V^{V} and structures were reported for vanabins, haloperoxidases, nitrate reductases, phosphatases, kinases, phosphodiesterases, phosphomutases, ATPases, ATP synthases, topoisomerases, ribonucleases, and ribozymes.⁶ In contrast, the adducts V^{IV} –proteins are rarely available and, to the best of our

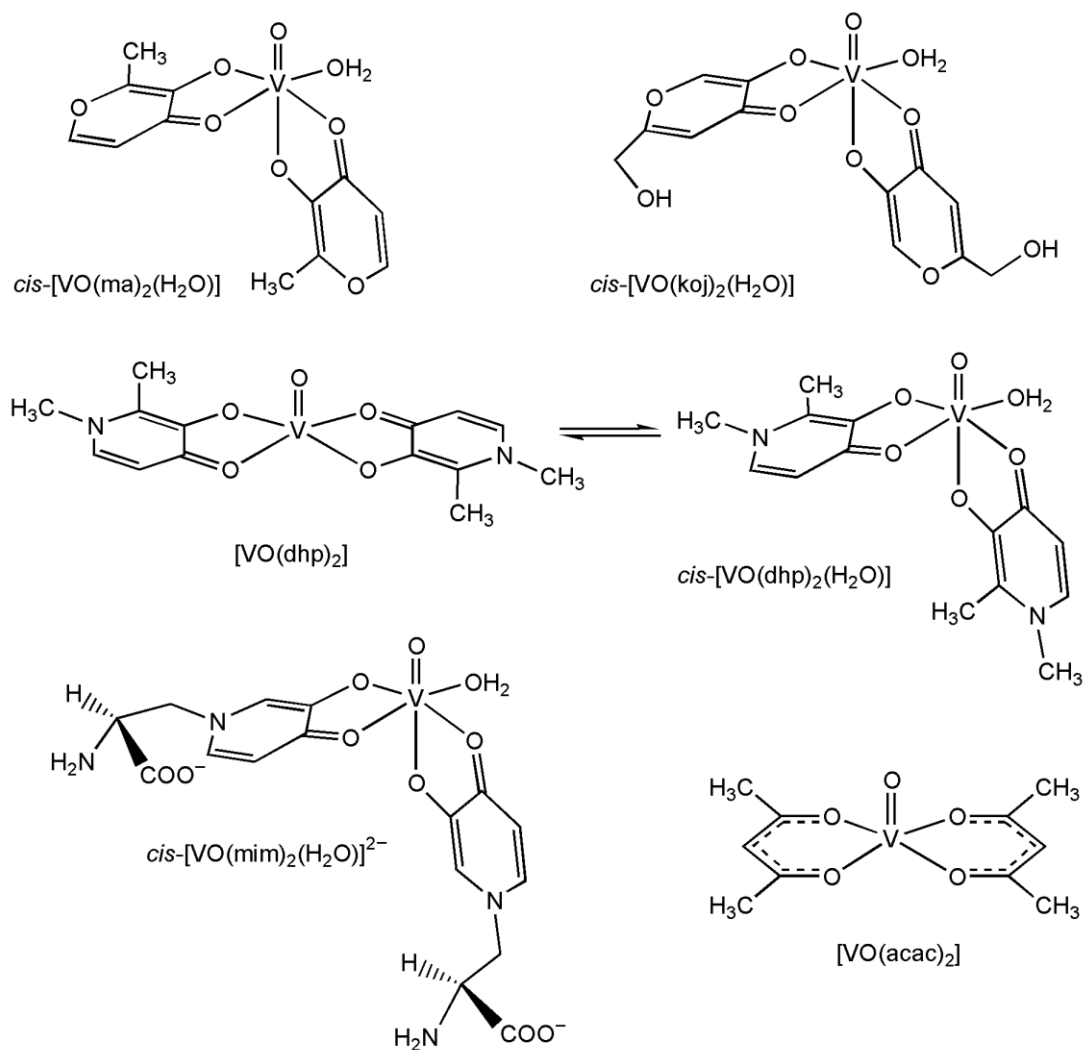
knowledge, only the XRD analyses for the species $[V^{IV}O(\text{picolinato})_2]\text{-lysozyme}^{9g}$ and, recently, $[V^{IV}O^{2+}]\text{-}(cytochrome\text{ }cb_{562})^{19}$ were described. For this reason and since a single crystal X-ray structure could not necessarily reflect the speciation in solution, alternative strategies to reach a complete description of the systems with vanadium(IV) must be adopted.

Dealing with V^{IV} compounds, EPR gives insights into the identity of equatorial donors bound to $V^{IV}O^{2+}$ ion because the value of the ^{51}V hyperfine coupling constant along the z axis (A_z) depends on the electron donor capacity of the ligands. ESI (ElectroSpray Ionization) and MALDI (Matrix-Assisted Laser Desorption/Ionization) represent the most powerful mass spectrometries (MS) to explore metallodrug–protein interactions. They give information on the number and stoichiometry of the metal–protein adducts formed,^{20, 21} and ESI-MS in particular has been used to study the reactivity of metallodrugs – among which cisplatin and its derivatives – with low molecular mass (amino acids, oligonucleotides and peptides) and high molecular mass biomolecules (proteins).²⁰⁻²² An important specificity of ESI-MS is that the metal concentration which can be used in the experiments falls in the range 10-100 μM , therefore very close to the physiological conditions.^{1,3}

Since EPR and ESI-MS do not allow identifying the exact region of the protein where the metal is bound, the specific amino acid residues involved in the coordination nor the possible stabilization of the adducts through secondary interactions such as hydrogen bonds and van der Waals contacts, the information provided by these techniques can be completed by computational methods and, particularly, docking calculations. Recently, our groups developed a computational procedure to predict the active binding between a metal and a protein (i.e. the coordination bond formation), including this contribution in the GoldScore scoring function of Gold software.²³ The framework has been recently validated on more than sixty X-ray characterized metallospecies with one or more coordination bonds.^{16, 23b} The results can be further improved by QM/MM or full QM cluster simulations.¹⁶

In the present study this approach was applied to the interaction of ubiquitin (Ub) with $V^{IV}O^{2+}$ ion and five $V^{IV}O$ compounds with potential pharmacological application as antidiabetic and anticancer

agents:^{1, 5, 24, 25} *cis*-[VO(ma)₂(H₂O)], *cis*-[VO(koj)₂], [VO(acac)₂], [VO(dhp)₂], and *cis*-[VO(mim)₂(H₂O)]²⁻, where ma, koj, acac, dhp, and mim stand for maltolate, kojate, acetylacetonate, 1,2-dimethyl-3-hydroxy-4(1*H*)-pyridinonate, and L-mimosinate (Scheme 1). Ubiquitin (Ub) is a small regulatory protein, ubiquitous in all the eukaryotes, with a polypeptide chain of 76 amino acids and a molecular weight of ca. 8.5 kDa.²⁶ It contains only few potential binding donors, including the *N*-terminal Met1 (S donor), His68 (N donor) as well as five carboxylates belonging to Asp and six to Glu residues (O donors).²⁰ Ub is commercially available with a high level of purity and its amino acid sequence is known in detail,²⁰ and for this reason it has been considered as a good model for studying metallodrugs–protein binding interactions. The interaction of ubiquitin with several antitumor species such as cisplatin and its derivatives,^{20, 22, 26} and some ruthenium and gold compounds,^{21, 27} was reported in the literature, but up to now there are no studies concerning the binding with vanadium compounds. Therefore, the results of the present paper could give new insights into the interaction of pharmacologically active V compounds with proteins, their speciation and the identity of the active species in the organism. Finally, the data presented could pave the way for a rational design of new pharmacologically active compounds, highlighting a series of features that must be tuned to optimize the interaction strength with the target protein(s).



Scheme 1. Structure of the five $V^{IV}O$ complexes in aqueous solution at physiological pH.

Experimental and Computational Section

Chemicals. Water was deionized prior to use through the purification system Millipore MilliQ Academic or purchased from Sigma-Aldrich (LC-MS grade). $V^{IV}O^{2+}$ solutions were prepared from $VOSO_4 \cdot 3H_2O$ following literature methods.²⁸ 3-Hydroxy-2-methyl-4*H*-pyran-4-one or maltol (Hma), 5-hydroxy-2-(hydroxymethyl)-4*H*-pyran-4-one or kojic acid (Hkoj), acetylacetonate (Hacac), 1,2-dimethyl-3-hydroxy-4(1*H*)-pyridinone (Hdhp), 2-amino-3-(3-hydroxy-4-oxo-1,4-dihydropyridin-1-yl)-propanoic acid or L-mimosine (H₂mim), 1-methylimidazole (MeIm) and 4-(2-

hydroxyethyl)piperazine-1-ethanesulfonic acid (HEPES) were Sigma-Aldrich products of the highest grade available and used as received.

Ubiquitin (Ub) from bovine erythrocytes was purchased from Sigma-Aldrich with code U6253.

The neutral solid compounds [VO(ma)₂] and [VO(dhp)₂] were synthesized according to the procedures established in the literature.^{29, 30, 31} [VO(acac)₂] was a Sigma-Aldrich compound.

EPR measurements. The solutions for EPR measurements were prepared by dissolving VOSO₄·3H₂O and ligands in ultra-pure water in order to get a V^{IV}O²⁺ concentration of 1.0 × 10⁻³ M and a metal-to-ligand molar ratio of 1/2 (for all the systems) and 1/1 (for ma, koj and acac only). Argon was bubbled through the solutions to ensure the absence of oxygen and avoid the oxidation of V^{IV}O²⁺ ion. To the solutions, HEPES buffer of 1.0 × 10⁻¹ M concentration was added.

The value of pH was raised to 7.4 and, to 1 mL of the solutions with the V species, Ub was added to obtain a concentration of 1.0 × 10⁻³ M and an initial molar ratio (V complex)/Ub of 1/1. Subsequently, various aliquots of the solution with V complex were added to have an Ub concentration between 6.25 × 10⁻⁵ M and 5.0 × 10⁻⁴ M and ratio (V complex)/Ub between 2/1 and 4/1. For measurements on the systems with metal-to-ligand molar ratio of 1/1, the pH was adjusted to the desired value with diluted NaOH or H₂SO₄ solutions before the solubilization of the protein.

EPR spectra were recorded at 120 or 298 K with an X-band Bruker EMX spectrometer equipped with a HP 53150A microwave frequency counter. The microwave frequency was 9.40-9.41 GHz at 120 K and 9.83-9.84 GHz at 298 K. When the samples were transferred into the EPR tubes, the spectra were immediately measured. Signal averaging was used to increase the signal to noise ratio.³²

The model systems V^{IV}O²⁺/L and V^{IV}O²⁺/L/MeIm, where L = ma, koj, acac, dhp and mim, were considered to study the binding of V^{IV}O species to Ub.

ESI-MS measurements. The solutions for ESI-MS measurements were prepared by dissolving the solid complexes [VO(ma)₂], [VO(acac)₂] and [VO(dhp)₂] in LC-MS grade water to obtain a V concentration of 1.0-2.0 × 10⁻³ M. In the system with kojate and L-mimosine, VOSO₄·3H₂O (1.0-

2.0×10^{-3} M) and the ligand (koj or mim) were dissolved in LC-MS grade water to have a metal-to-ligand ratio of 1/2 and a stoichiometric amount of $\text{BaCl}_2 \cdot 2\text{H}_2\text{O}$ was added to remove the interfering sulphate ion as BaSO_4 . Subsequently, all the solutions were diluted in LC-MS grade water with an aliquot of a stock ubiquitin solution (500 μM) to obtain a (V complex)/Ub ratio of 3/1, 5/1 and 10/1 and a protein concentration of 5 μM . Argon was bubbled during all the operations to avoid the $\text{V}^{\text{IV}}\text{O}^{2+}$ oxidation. ESI-MS spectra were recorded immediately after the preparation of the solution.

Mass spectra in the positive-ion mode were obtained on a Q Exactive™ Plus Hybrid Quadrupole-Orbitrap™ (Thermo Fisher Scientific) mass spectrometer. The solutions were infused at a flow rate of 5.00 $\mu\text{L}/\text{min}$ into the ESI chamber. The spectra were recorded in the m/z range 300-4500 at a resolution of 140,000 and accumulated for at least 5 min in order to increase the signal-to-noise ratio. The instrumental conditions used for the measurements were as follows: spray voltage 2300 V, capillary temperature 250 °C, sheath gas 10 (arbitrary units), auxiliary gas 3 (arbitrary units), sweep gas 0 (arbitrary units), probe heater temperature 50 °C. ESI-MS spectra were analyzed by using Thermo Xcalibur 3.0.63 software (Thermo Fisher Scientific) and the average deconvoluted monoisotopic masses were obtained through the Xtract tool integrated in the software.

DFT and Docking Calculations. All the DFT calculations were carried out with Gaussian 09 (revision D.01).³³ The $\text{V}^{\text{IV}}\text{O}$ complexes geometries and harmonic frequencies were computed at the level of theory B3P86/6-311g(d,p) using the SMD model³⁴ for water. This guarantees a good degree of accuracy in the structure optimization of first-row transition metal complexes³⁵ and, particularly, of vanadium compounds.³⁶

The calculation of the ^{51}V hyperfine coupling constants (A) was performed on the optimized structures at BHandHLYP/6-311+g(d) level of theory, according to the procedures previously published.³⁷ The theory background can be found by the interested readers in refs.³⁸. The values of A_z were reported as the absolute values, following the usual formalism in the literature.

Docking calculations were carried out through GOLD 5.2 software³⁹ on the X-ray structure available in the Protein Data Bank (PDB) of ubiquitin (PDB code: 3H1U⁴⁰). The PDB structure

was cleaned removing all the small molecules and crystallographic waters, and hydrogen atoms were added with the UCSF Chimera program.⁴¹ The protonation state of the amino acid side chains was computed by means of PROPKA algorithm.⁴² Concerning the metallospecies, the DFT optimized structures were preliminary treated replacing the equatorial leaving ligands (four water molecules for $[\text{VO}(\text{H}_2\text{O})_4]^{2+}$, one equatorial H_2O for *cis*- $[\text{VO}(\text{ma})_2(\text{H}_2\text{O})]$ and two for $[\text{VO}(\text{ma})(\text{H}_2\text{O})_2]^+$, $[\text{VO}(\text{koj})(\text{H}_2\text{O})_2]^+$ and $[\text{VO}(\text{acac})(\text{H}_2\text{O})_2]^+$) with dummy hydrogen atoms according to what was recently established.^{16, 23} All dockings were computed considering the possible dihedral changes along the ligand aliphatic bonds applying the GOLD algorithm. The solutions were analyzed by means of GaudiView.⁴³

To identify the possible Ub binding sites for the $\text{V}^{\text{IV}}\text{O}$ species, relative Solvent Excluded Surface (SES) calculations⁴⁴ were preliminarily performed focusing on the most exposed potential coordinating residues. For the dockings of bare $\text{V}^{\text{IV}}\text{O}^{2+}$ ion and $\text{VO}(\text{ma})^+$, $\text{VO}(\text{koj})^+$ and $\text{VO}(\text{acac})^+$ moieties, the protein space was first probed for the zones where at least two potential coordinating residues (Asp, Glu, Asn, Gln and His) featured a β -carbon within a distance of 2.5 Å from each queried grid point. Both the protonation states at δ and ϵ nitrogens of His imidazole ring were considered during the simulations.

The docking simulations were carried out constructing in the region of interest an evaluation sphere of 12 Å. For the classical dockings the whole rigid protein was considered, while side chains flexibility was taken into account considering the GOLD implemented rotamers libraries.⁴⁵ Genetic algorithm (GA) parameters have been set to 50 GA runs and a minimum of 100,000 operations. The other parameters of GA were set to default.

The scoring (*Fitness* of GoldScore) was evaluated applying the modified version of GoldScore scoring function, which was validated in previously published papers.^{16, 23} The best solutions (binding poses) were evaluated through three main criteria: i) the mean (F_{mean}) and the highest value (F_{max}) of the scoring (*Fitness* of GoldScore) associated with each pose; ii) the population of the cluster containing the best pose; iii) the position in the *Fitness* ranking of the computed cluster.

The refinement of the $V^{IV}O^{2+}$ -Ub adduct found by dockings was performed cutting out the region with the $V^{IV}O^{2+}$ ion, and neighbor interacting amino acid side chains and freezing the backbone atoms as reported by Siegbahn and Himo.⁴⁶ The resulting clusters contain 54, 43 and 44 atoms for the models of the sites **1**, **2** and **3**, respectively. The geometry relaxation and ΔE calculations were performed at B3P86/6-311++g(d,p) level of theory within the framework of SMD model³⁴ for water.

Results and Discussion

Binary system $V^{IV}O^{2+}$ /Ub. The EPR spectrum recorded on the binary system $V^{IV}O^{2+}$ /Ub with a ratio 1/1 was reported in the trace a of Figure 1 and consists of only one set of resonances with $g_z = 1.941$ and $A_z = 168.8 \times 10^{-4} \text{ cm}^{-1}$ (indicated with **Ia** in trace a). This was compared with those obtained in the system with hemoglobin (Hb) (traces b and c of Figure 1), where the presence of the two sites α and β ⁴⁷ (**Ib** and **Iib** in Figure 1) was revealed.

The comparison of the data indicates that the spectrum of **Ia** is similar to that of the site α of hemoglobin (**Ib**) for which the binding of COO^- groups of Glu and Asp to the $V^{IV}O^{2+}$ ion was proposed with water molecules occupying the remaining equatorial positions.⁴⁷ The values of A_z are comparable (it is $168.8 \times 10^{-4} \text{ cm}^{-1}$ for **Ia** and $170.1 \times 10^{-4} \text{ cm}^{-1}$ for **Ib** of Hb⁴⁷); in contrast, A_z measured for Ub is very different from the site β of Hb (**Iib**), in which the coordination of a His-N adds to that of Asp/Glu-COO, lowering the value of the hyperfine coupling constant to $166.8 \times 10^{-4} \text{ cm}^{-1}$ ⁴⁷. This analysis would indicate that the only one His residue (His68) of Ub is scarcely available for the $V^{IV}O^{2+}$ coordination or that its binding is not assisted by other strong donors, unlike what happens with Hb. The larger number of Asp and Glu residues in ubiquitin (five and six, respectively⁴⁸) would suggest that the coordination of COO^- groups is more likely than that of His68.

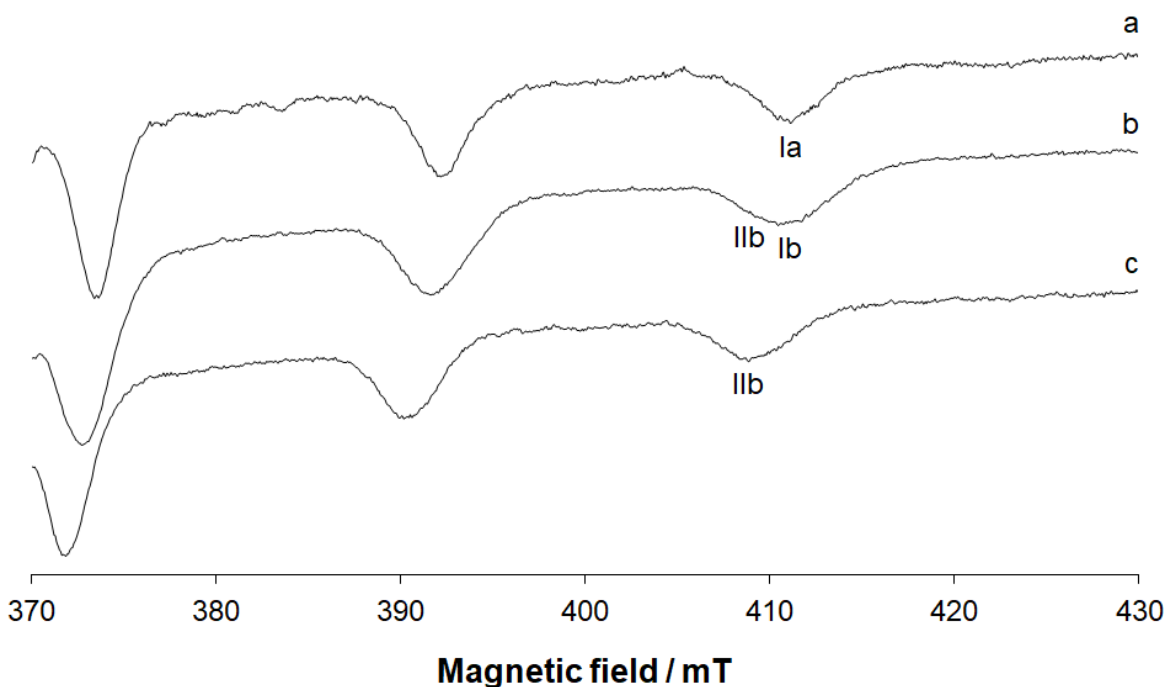


Figure 1. High field region of the EPR spectra recorded on frozen solutions (120 K) containing: a) $V^{IV}O^{2+}/Ub$ 1/1 ($V^{IV}O^{2+}$ 1.0×10^{-3} M, pH 7.4); b) $V^{IV}O^{2+}/Hb$ 2/1 ($V^{IV}O^{2+}$ 6.2×10^{-4} M, pH 6.3); c) $V^{IV}O^{2+}/Hb$ 2/1 ($V^{IV}O^{2+}$ 6.2×10^{-4} M, pH 5.0). The $M_I = 7/2$ resonance of the binding site of Ub is indicated with **Ia**, while those of the sites α and β of Hb with **Ib** and **IIb**.

To identify the $V^{IV}O^{2+}$ binding sites and the specific residues involved in the metal coordination, a multiscale computational approach was applied consisting of: i) an exploratory study of the protein structure looking for the regions satisfying the coordination criteria suggested by the EPR; ii) a docking assay on the identified regions and iii) a full quantum mechanics (QM) relaxation of the predicted structures followed by a DFT simulation of the EPR spin Hamiltonian parameters.

The results, summarized in Table 1, suggest that ubiquitin has three potential binding sites (indicated with **1**, **2** and **3** in this study): the first two involve two carboxylate donors, Glu16/Glu18 and Glu24/Asp52, and the third one includes the unique histidine of protein (His68) and two keto donors of the backbone belonging to Thr7 and Leu69 (Figure 2). The docking assay indicates that **1**

is the strongest site with F_{\max} and F_{mean} higher than 40 GoldScore units and a cluster population of 48/50 solutions. The $\text{V}^{\text{IV}}\text{O}^{2+}$ ion is coordinated by Glu16 and Glu18, the remaining equatorial positions being occupied by two water molecules (Figure 2a); the hydrogen bond between ϵ -amino of Lys29 and V=O group stabilizes this interaction. The potential site 2 is characterized by the coordination of carboxylates of Glu24 and Asp52, with the other two equatorial sites presumably occupied by two H_2O ; the values of the scoring fitness F_{\max} and F_{mean} for this site are ca. 14 GoldScore units smaller than those of site 1 and the population of the cluster is 26/50 (Figure 2b). The low GoldScore value for the site 3 indicates a low stability of this environment, in agreement with the EPR data that exclude His coordination.

Table 1. Binding sites for $\text{V}^{\text{IV}}\text{O}^{2+}$ ion to Ub determined by docking methods.

Site	Residues	Coordination	V–N ^a	V–O ^a	F_{\max} ^b	F_{mean} ^c	Pop. ^d	Rank. ^e
1	Glu16; Glu18	COO; COO; 2H ₂ O	–	2.318; 2.096, 2.789 ^f	44.8	42.8	48/50	I
2	Glu24; Asp52	COO; COO, 2H ₂ O	–	1.902, 2.637	30.5	28.1	26/50	I
3	Thr7; His68; Leu69	CO; N; CO; H ₂ O	2.216	2.454, 2.792	25.1	25.0	46/50	I

^a Distance between V and protein donors in Å. ^b GoldScore *Fitness* value obtained for the most stable pose of each cluster (F_{\max}). ^c Average value of GoldScore *Fitness* for each cluster (F_{mean}). ^d Population of the cluster (numbers of solutions per cluster). ^e Ranking of the identified cluster.

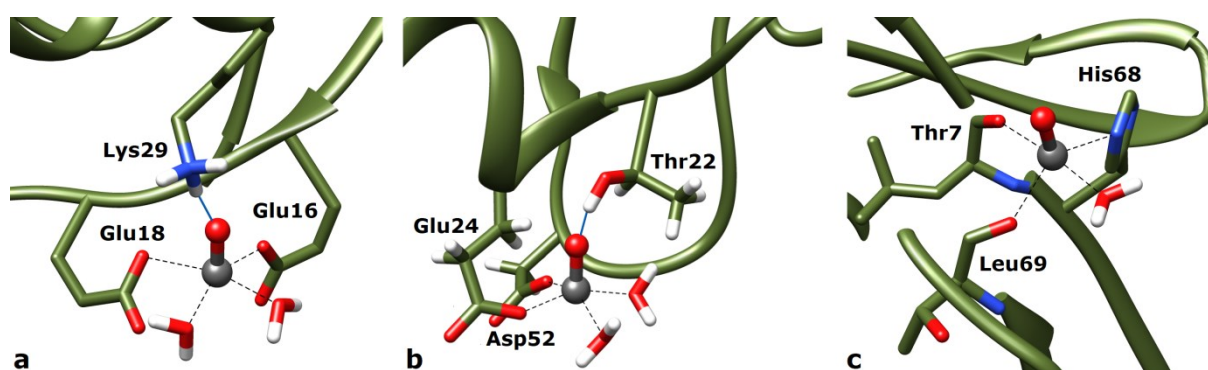


Figure 2. Potential binding sites of Ub for the $\text{V}^{\text{IV}}\text{O}^{2+}$ ion on the basis of the docking calculations: (a) site 1; (b) site 2 and (c) site 3. The hydrogen bonds are highlighted with the full blue lines.

QM calculations on the three sites lead to a significant refinement of the geometry (Table 2) and the bond distances approach those expected for V–N(imidazole), V–O(carboxylate) and V–O(water).⁴⁹ The optimization of the three sites found by dockings was performed cutting out the region containing the $V^{IV}O^{2+}$ ion and the interacting amino acid side chains and freezing the backbone atoms as reported by Siegbahn and Himø (see Experimental and Computational Section).⁴⁶ The computed ΔE values for the formation of the three sites indicate that the stability order is: site **1** ~ site **2** \gg site **3**. Furthermore, the experimental A_z value was compared with those calculated by DFT methods for sites **1-3**; the percent deviations suggest that the value calculated for the site **1** is that closer to the experimental one.

Summarizing the docking and QM results, the site **1** should be slightly more stable than site **2** and much more stable than site **3**. Therefore, it is expected that the under our experimental conditions, the site **3** is not populated at all, while the ion $V^{IV}O^{2+}$ would distribute between the sites **1** and **2**, with **1** being slightly more populated than **2**.

Table 2. Binding sites for $V^{IV}O^{2+}$ ion to Ub refined by QM methods and comparison between the experimental and calculated (with DFT methods) A_z values.

Site	V–N ^a	V–O ^a	V–OH ₂ ^a	ΔE ^b	A_z^{exptl} ^c	A_z^{calcd} ^c	PD (A_z) ^d
1	–	1.991, 1.968	2.036, 2.080	-30.8	168.8	164.1	-2.8
2	–	1.936, 1.956	2.095, 2.085	-31.5	168.8	175.3	3.9
3	2.039	1.996, 2.026	2.071	-13.7	168.8	180.7	7.1

^a Distance between V and protein donors in Å. ^b ΔE (in kcal mol⁻¹) calculated for the reactions $[VO(H_2O)_4]^{2+} + \text{site } \mathbf{1} \rightleftharpoons VO(\text{site } \mathbf{1})(H_2O)_2 + 2H_2O$, $[VO(H_2O)_4]^{2+} + \text{site } \mathbf{2} \rightleftharpoons VO(\text{site } \mathbf{2})(H_2O)_2 + 2H_2O$, and $[VO(H_2O)_4]^{2+} + \text{site } \mathbf{3} \rightleftharpoons VO(\text{site } \mathbf{3})(H_2O) + 3H_2O$, respectively. ^c A_z in 10^{-4} cm⁻¹. ^d Percent deviation (PD) of the calculated values, $|A_z|^{\text{calcd}}$, from the absolute experimental ones, $|A_z|^{\text{exptl}}$, obtained with the formula: $[(|A_z|^{\text{calcd}} - |A_z|^{\text{exptl}}) / |A_z|^{\text{exptl}}] \times 100$.

Ternary system V^{IV}O²⁺/ma/Ub. Maltol (ma) is a naturally occurring compound and has been approved as a food additive in many countries.⁵⁰ Its complex with V^{IV}O²⁺ ion, bis(maltolato)oxidovanadium(IV) (BMOV), is considered the benchmark V based antidiabetic agent for comparison with other compounds. Its derivative, bis(ethylmaltolato)oxidovanadium(IV) (BEOV) was the first V complex subjected to clinical trials (it underwent Phase 1 and 2),⁵¹ but the tests have been suspended for the expiry of the patent in 2011.^{5, 25} In an aqueous solution, the solid square pyramidal species [VO(ma)₂] undergoes a structural rearrangement to *cis*-[VO(ma)₂(H₂O)] (Scheme 1), which is the major species at physiological pH, with a water molecule in the equatorial plane in the *cis* position to V=O bond.^{52, 53}

In this study, EPR spectra on the ternary system containing V^{IV}O²⁺, ma and Ub at physiological pH and ratio (V^{IV}O complex)/Ub of 1/1, 2/1 and 4/1 were recorded. The spectra show the presence of three species (indicated with **I**, **III** and **IV** in Figure 3). The species **III** is characterized by $g_z = 1.949$ and $A_z = 164.9 \times 10^{-4} \text{ cm}^{-1}$ and its formula **can be indicated** with VO(ma)₂(His-N) in which the imidazole-N of His68 replaces the equatorial water molecule of *cis*-[VO(ma)₂(H₂O)] (indicated with **I**); in fact, the EPR parameters are very similar to those of the model species *cis*-[VO(ma)₂(MeIm)] ($g_z = 1.948$ and $A_z = 164.8 \times 10^{-4} \text{ cm}^{-1}$, **II**^{8e}). However, the broad resonances around 410 mT, corresponding to the $M_1 = 7/2$ transition, suggest that other species exist in solution, **whose importance increases with increasing** the ratio (V^{IV}O complex)/Ub. The resonance indicated with **IV** belongs to an additional mixed species VO(ma)₂(Asp/Glu-COO), revealed from ratio 1/1 to 2/1, in which the fourth equatorial position of the moiety *cis*-VO(ma)₂ is occupied by carboxylate groups of Asp and Glu residues that cause a slight increase in the A_z value in comparison with the His-N coordination of **III** (in fact, the 'additivity relationship' attribute a contribution of $40.7 \times 10^{-4} \text{ cm}^{-1}$ to an imidazole-N and $42.1 \times 10^{-4} \text{ cm}^{-1}$ to a carboxylate-O⁵⁴). The intensity of the resonances of **IV** increases compared to **III** at ratio 2/1, suggesting that at least two carboxylate groups belonging to Asp or Glu residues interact with V. When the ratio (V^{IV}O complex)/Ub becomes 4/1

the $M_1 = 7/2$ resonances shift to higher field, indicating that no more ubiquitin residues are available for the V binding and the excess of $V^{IV}O^{2+}$ remains in solution as *cis*-[VO(ma)₂(H₂O)] (**I**). Therefore, the general formula of the species formed is 3[VO(ma)₂]-Ub.

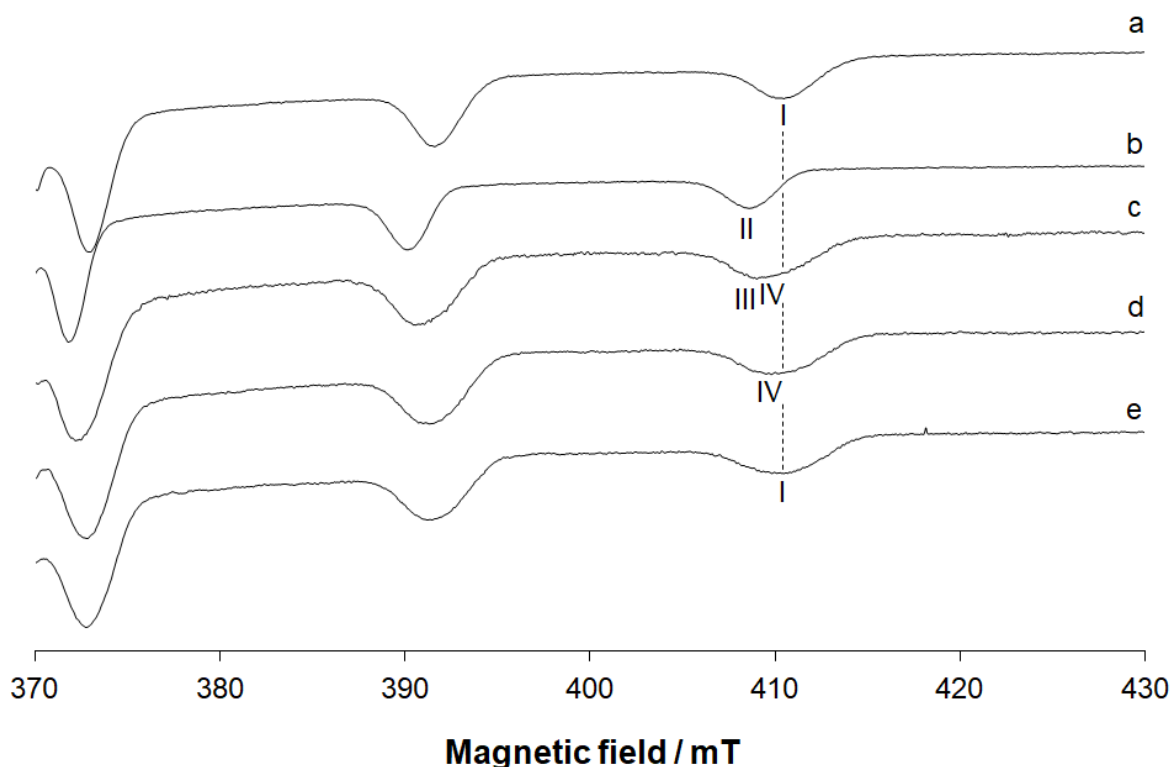


Figure 3. High field region of the EPR spectra recorded on frozen solutions (120 K) containing: a) $V^{IV}O^{2+}/ma$ 1/2; b) $V^{IV}O^{2+}/ma/1-MeIm$ 1/2/4; c) $V^{IV}O^{2+}/ma/Ub$ 1/2/1; d) $V^{IV}O^{2+}/ma/Ub$ 2/4/1; e) $V^{IV}O^{2+}/ma/Ub$ 4/8/1. $V^{IV}O^{2+}$ concentration was 1.0×10^{-3} M and pH was 7.4 in all the systems. The $M_1 = 7/2$ resonance of the adducts VO(ma)₂(His-N) is indicated with **III** and of VO(ma)₂(Asp/Glu-COO) with **IV**. **I** and **II** indicate the $M_1 = 7/2$ resonances of *cis*-[VO(ma)₂(H₂O)] and *cis*-[VO(ma)₂(MeIm)], respectively. The resonance of the species present in the binary species, *cis*-[VO(ma)₂(H₂O)], is also denoted with the dotted line.

To complement the EPR data, docking calculations were carried out to characterize the adducts between $V^{IV}O$ moiety and ubiquitin. The first simulations were carried out to ascertain the Ub binding to the fragment $cis\text{-VO}(\text{ma})_2$; for this reason, the structures of the eight possible isomers $OC\text{-}6$ for $cis\text{-}[\text{VO}(\text{ma})_2(\text{H}_2\text{O})]$ (i.e., the Δ and Λ series of $OC\text{-}6\text{-}34$, $OC\text{-}6\text{-}32$, $OC\text{-}6\text{-}23$ and $OC\text{-}6\text{-}24$ ^{23a}) were DFT optimized and the fourth equatorial position activated as described in the Experimental and Computational Section. The docking assay was based on the hypothesis suggested by EPR, and the regions of protein containing accessible nitrogen and oxygen donors were explored. The results, similarly to what was found with previously studied systems^{9g, 23a}, show that the binding affinity depends on the specific isomer under examination. Based on the GoldScore *Fitness* and cluster population analysis (Table 3), the isomers with the highest affinity for Ub are $OC\text{-}6\text{-}23\text{-}\Delta$, $OC\text{-}6\text{-}23\text{-}\Lambda$ and $OC\text{-}6\text{-}32\text{-}\Delta$ and the relative binding affinity of the residues can be summarized as Asp21 >> Glu18 > His68 >> Glu16. It must be highlighted that, due to their spatial proximity, Asp21 and Glu18 cannot simultaneously bind two $cis\text{-VO}(\text{ma})_2$ moieties. The most stable adducts formed by the isomer $OC\text{-}6\text{-}23\text{-}\Delta$ are shown in Figure 4. It can be noted that the binding of Asp21 and Glu18 is stabilized by a hydrogen bond between the oxygen atoms of the complex and the protonated ϵ -amino side chain of Lys29 (Figure 4, a and b).

These results allow us to rationalize the EPR data of the system $\text{VO}(\text{ma})_2/\text{Ub}$, postulating that the moiety $cis\text{-VO}(\text{ma})_2$ is distributed between the not independent residues Asp21 and Glu18 (resonance indicated with **IV** in Figure 3) and His68 (resonance indicated with **III**); **by increasing the ($V^{IV}O$ complex)/Ub ratio**, weaker sites such as Glu16 could participate to the binding justifying the broadening of the absorption around 410 mT observed at 4/1 ratio. Therefore, the formula $3[\text{VO}(\text{ma})_2]\text{-Ub}$ can be explained with the binding of three $cis\text{-VO}(\text{ma})_2$ moieties to Asp21 or Glu18, His 68 and Glu16.

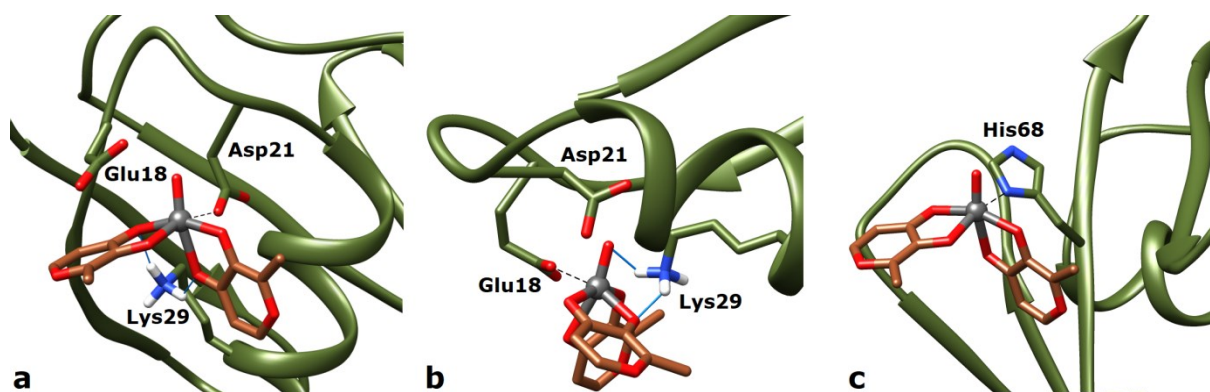


Figure 4. Most stable structures predicted by docking for the binding of *cis*-VO(ma)₂ to Ub: a) *OC*-23- Δ -VO(ma)₂ to Asp21; b) *OC*-23- Δ -VO(ma)₂ to Glu18; c) *OC*-23- Δ -VO(ma)₂ to His68. The hydrogen bonds are highlighted with the full blue lines.

Table 3. Docking solutions for the interaction of the moiety *cis*-VO(ma)₂ with Ub.

Enantiomer	Residues	V-X ^a	F_{\max} ^b	F_{mean} ^c	Pop. ^d	Rank. ^e
<i>OC</i> -6-23- Δ	Asp21	2.392	48.58	40.13	38/50	I
	Glu18	2.191	44.09	41.12	12/50	II
	His68	2.349	36.70	34.31	50/50	I
<i>OC</i> -6-23- Λ	Asp21	2.385	54.17	41.84	14/50	I
	Glu18	1.985	40.54	35.84	36/50	II
	His68	2.167	38.20	36.78	50/50	I
<i>OC</i> -6-24- Δ	Asp21	2.341	41.27	40.20	12/50	I
	Glu18	2.334	38.74	38.83	38/50	II
	His68	2.383	37.90	36.53	50/50	I
<i>OC</i> -6-24- Λ	Glu18	2.103	44.38	37.97	33/50	I
	Asp21	2.393	42.18	36.06	12/50	II
	His68	2.245	39.69	36.51	50/50	I
<i>OC</i> -6-32- Δ	Asp21	2.218	51.44	41.71	31/50	I
	Glu18	2.052	42.27	41.80	19/50	II

	His68	2.232	34.43	32.91	50/50	I
OC-6-32- Δ	Glu18	2.151	38.00	35.79	49/50	I
	Glu16	3.147	37.37	–	1/50	II
	His68	2.346	38.70	37.67	50/50	I
OC-6-34- Δ	Glu18	2.278	42.06	39.55	50/50	I
	His68	2.146	37.33	32.96	49/50	I
OC-6-34- Λ	Glu18	1.966	43.72	37.10	41/50	I
	His68	2.278	39.38	37.56	50/50	I

^a Distance in Å (X = O for Glu16, Glu18 and Asp21, and N for His68). ^b GoldScore *Fitness* value obtained for the most stable pose of each cluster (F_{\max}). ^c Average value of GoldScore *Fitness* for each cluster (F_{mean}). ^d Population of the cluster (numbers of solutions per cluster). ^e Ranking of the identified cluster.

To evaluate which adducts are formed at low V concentration (15-50 μM), ESI-MS spectra of the system with *cis*-[VO(ma)₂(H₂O)] and ubiquitin were recorded in ultrapure water varying the molar ratio between the complex and the protein (3/1, 5/1 and 10/1). The spectrum of free ubiquitin was recorded as a reference and is characterized by a series of peaks corresponding to the different charged states of protein from +5 to +10. In the deconvoluted spectrum (Figure S1) it is possible to observe the main signal corresponding to the mass of ubiquitin at 8564.6 Da and the series of signals due to adducts between the protein and ubiquitinary ions like Na⁺ and K⁺. The isotopic pattern of the peak corresponding to the charge +9 of protein allowed us to confirm the molecular formula of ubiquitin reported in the literature (C₃₇₈H₆₃₀N₁₀₅O₁₁₈S).⁵⁵ In the spectra recorded in the system with maltol, the peaks at higher mass values than 8564.6 Da (the free protein) suggest the formation of protein–(metal species) adducts (Figure 5). When the protein concentration is 5 μM the species $n[\text{VO(ma)}]\text{–Ub}$ are observed with the value of n depending on the molar ratio used: $n = 1$ when the ratio is 3/1 and $n = 2$ when it is 5/1 and 10/1. The experimental isotopic pattern of the peak corresponding to the species [VO(ma)]–Ub was simulated and the results indicate the molecular

formula $C_{384}H_{635}O_{122}N_{105}SV$ with $m/z = 1248.1$ and $z = 7$ (Figure S2). The adducts observed in aqueous solution after the interaction of *cis*-[VO(ma)₂(H₂O)] with Ub are listed in Table 4.

Table 4. Main adducts formed after the interaction of the VOL₂ complexes with Ub revealed with ESI-MS.

System	Adduct	V ^{IV} O/Ub	Mass (Da)
VO(ma) ₂ /Ub	V ^V O ₂ ⁺	3/1, 5/1, 10/1	8646.6
	[VO(ma)]–Ub	3/1, 5/1, 10/1	8755.6
	2[VO(ma)]–Ub	5/1, 10/1	8946.6
	3[VO(ma)]–Ub	10/1	9137.5
VO(koj) ₂ /Ub	[VO(koj)]–Ub	5/1, 10/1	8771.6
	2[VO(koj)]–Ub	10/1	8977.5
VO(acac) ₂ /Ub	[VO(acac)]–Ub	3/1, 5/1, 10/1	8729.6
	2[VO(acac)]–Ub	3/1, 5/1, 10/1	8894.6
	3[VO(acac)]–Ub	3/1, 5/1, 10/1	9059.5
VO(dhp) ₂ /Ub	[VO(dhp)]–Ub	3/1, 5/1, 10/1	8768.6
	[VO(dhp) ₂]–Ub	3/1, 5/1, 10/1	8907.7
VO(mim) ₂ /Ub	[VO(mim)]–Ub	3/1, 5/1, 10/1	8827.6
	[VO(mim) ₂]–Ub	3/1, 5/1, 10/1	9025.7
	2[VO(mim) ₂]–Ub	10/1	9486.7

It is interesting to notice that in all the spectra the additional peak due to the adduct of Ub with V^VO₂⁺ (8646.6 Da) is revealed; the experimental isotopic pattern of this peak was simulated as well and corresponds to a species with molecular formula $C_{378}H_{630}N_{105}O_{120}SV$, i.e. [V^VO₂]⁺–Ub ($m/z = 1236.2$ and $z = 7$, see Figure S3).

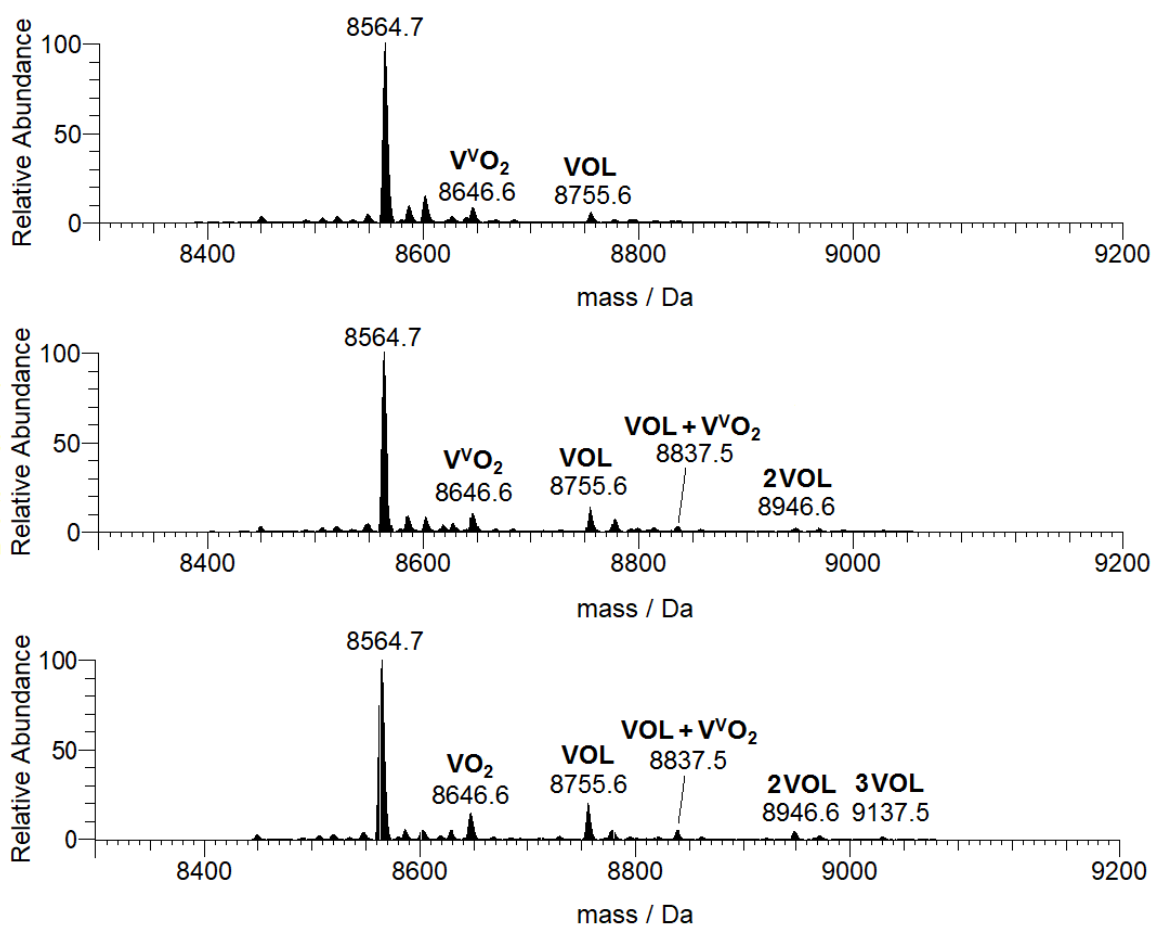


Figure 5. Deconvoluted ESI-MS spectra recorded on the system containing $\text{VO}(\text{ma})_2$ and ubiquitin ($5 \mu\text{M}$) with molar ratio 3/1 (top), 5/1 (centre) and 10/1 (bottom). With VOL and VVO_2 the fragments $\text{VO}(\text{ma})^+$ and VVO_2^+ that interact with Ub are indicated.

Three comments can be made on these results: i) the hydrolysis of $\text{cis-}[\text{VO}(\text{ma})_2(\text{H}_2\text{O})]$ at low V concentration ($15, 25$ and $50 \mu\text{M}$ in Figure 5) favors the formation of mono-chelated $[\text{VO}(\text{ma})(\text{H}_2\text{O})_2]^+$ species and ubiquitin binds up to two fragments $\text{VO}(\text{ma})^+$ probably with the contemporaneous coordination of two residue side-chains which replace the two adjacent water molecules; ii) the aquaion of $\text{V}^{\text{IV}}\text{O}^{2+}$, partially formed at low V concentration upon the hydrolysis,

binds to Ub through the residues Glu16 and Glu18 (see the section System $V^{IV}O^{2+}/Ub$ and Figure 2) and – as pointed out in the literature ⁵⁶ and verified for other $V^{IV}O$ species ⁷ – it is probably oxidized in-source during the recording of the spectrum, giving the cation $V^{VO_2^+}$; iii) depending on the concentration and pH, other species like $VO(ma)(OH)$ or $(VO)_2(ma)_2(OH)_2$ may also be present in solution and their interaction with Ub cannot be ruled out.

In order to completely characterize the species revealed by ESI-MS, anisotropic EPR spectra were recorded as a function of pH using the molar ratio $V^{IV}O^{2+}/ma/Ub$ 1/1/1 (Figure 6, traces b, d, f) to favor the interaction of the mono-chelated complex $[VO(ma)(H_2O)_2]^+$ with ubiquitin. From the analysis of Figure 6, it is possible to observe the presence in aqueous solution of two adducts, one in the pH range 4.7-5.4 (indicated with **III**) and of another above pH 6.5 (**IV**). The formation of these two different species can be rationalized considering that at acidic pH values (when the imidazole-N of the histidines are in the protonated form and cannot interact with the metal ion) the two water molecules in the equatorial plane are replaced by carboxylate groups (**III**); the value of g_z and A_z for **III** ($g_z = 1.943$ and $A_z = 168.7 \times 10^{-4} \text{ cm}^{-1}$) confirm this attribution. The resonances indicated with **IV**, instead, coincide with those of *cis*- $[VO(ma)_2(MeIm)]$ (**V**), suggesting that around the neutrality the bis-chelated complex *cis*- $[VO(ma)_2(H_2O)]$ coexists with the species **III** and interacts with protein after the replacement of the equatorial water ligand by imidazole-N of His68 residue.

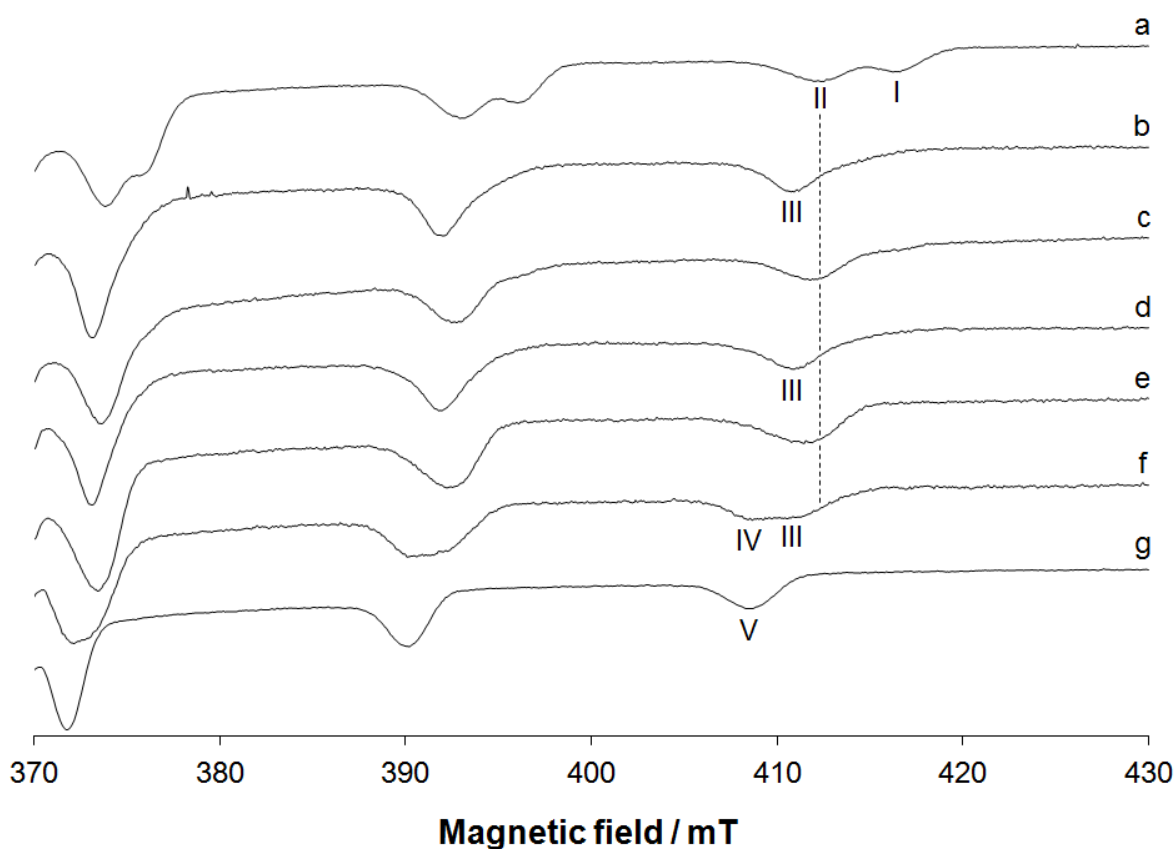


Figure 6. High field region of the EPR spectra recorded on frozen solutions (120 K) containing: a) $V^{IV}O^{2+}/ma$ 1/1 (pH 4.1); b) $V^{IV}O^{2+}/ma/Ub$ 1/1/1 (pH 4.7); c) $V^{IV}O^{2+}/ma$ 1/1 (pH 5.3); d) $V^{IV}O^{2+}/ma/Ub$ 1/1/1 (pH 5.4); e) $V^{IV}O^{2+}/ma$ 1/1 (pH 6.7); f) $V^{IV}O^{2+}/ma/Ub$ 1/1/1 (pH 6.5); g) $V^{IV}O^{2+}/ma/MeIm$ 1/2/4 (pH 7.4). $V^{IV}O^{2+}$ concentration was 1.0×10^{-3} M in all the systems. The $M_I = 7/2$ resonance of the adducts $VO(ma)(Asp/Glu-COO)_2$ are indicated with **III** and of $VO(ma)_2(His-N)$ with **IV**. **I**, **II** and **V** indicate the $M_I = 7/2$ resonances of $V^{IV}O^{2+}$ aquaion, $[VO(ma)(H_2O)_2]^+$ and *cis*- $[VO(ma)_2(MeIm)]$, respectively. The resonance of the major species present in the binary system, $[VO(ma)(H_2O)_2]^+$, is also denoted with the dotted line.

The interaction of the **mono-chelated** moiety $VO(ma)^+$, suggested by ESI-MS and EPR techniques, was also evaluated through docking calculations for *SPY-5-13-A* and *SPY-5-13-C* enantiomers, in which the two equatorial vacancies were activated for the Ub coordination. The

calculations were performed considering that in the pH range used in the EPR experiments (see Figure 6), histidines have two protonation states. From a PROPKA analysis,⁴² the His68 side chain is in its protonated form at acidic pH (4.7 and 5.4) and unable to coordinate V, while it is in the neutral form at pH 6.5 with the possibility to bind V through the imidazole-N.

The docking results indicate that four binding sites are possible with the simultaneous coordination of two amino acid side-chains: a primary site involving the coordination of Asp21 and Glu18 in which hydrogen bond stabilization between the oxygen atoms of the complex and the protonated ϵ -amino group of Lys29 is predicted (site 1', Figure 7a), a secondary binding site with vanadium coordinated by Glu16 and Glu18 with the formation of a similar hydrogen bond (site 1, Figure 7b), plus two other sites involving the coordination of the couples Glu24/Asp52 and Glu51/Asp52 (sites 2 and 2'). It must be noticed that the sites 1 and 2 are the same with which the $V^{IV}O^{2+}$ ion interacts (see Figure 2) and that 1 and 1' on one hand, and 2 and 2' on the other are not independent since the binding of $VO(ma)^+$ to one of them precludes that of a second moiety to the other site. Moreover, in contrast with the simulations for the bis-chelated species $VO(ma)_2$, the results suggest no particular chiral discrimination of the binding sites.

From an examination of the GoldScore *Fitness* and cluster population analysis (Table 5), it is reasonable to conclude that the adduct with the binding of Glu18 and Asp21 residues to $SPY-VO(ma)^+$ is strongly favored. The peaks observed in the ESI-MS spectra (Figure 5) and the $M_1 = 7/2$ resonances revealed by EPR spectroscopy (Figure 6) can be attributed to this species and to the analogous with the contemporaneous binding of Asp24 and Glu52 (or Glu51 and Glu52). The histidine residue, free to interact during the simulations, is not a possible donor for $VO(ma)^+$ moiety since other potential donors close to His68 are lacking. In this case the formula is $2[VO(ma)]-Ub$, as suggested by ESI-MS technique, with the binding of Glu18/Asp21 or Glu16/Glu18, and Glu24/Asp52 or Glu51/Asp52.

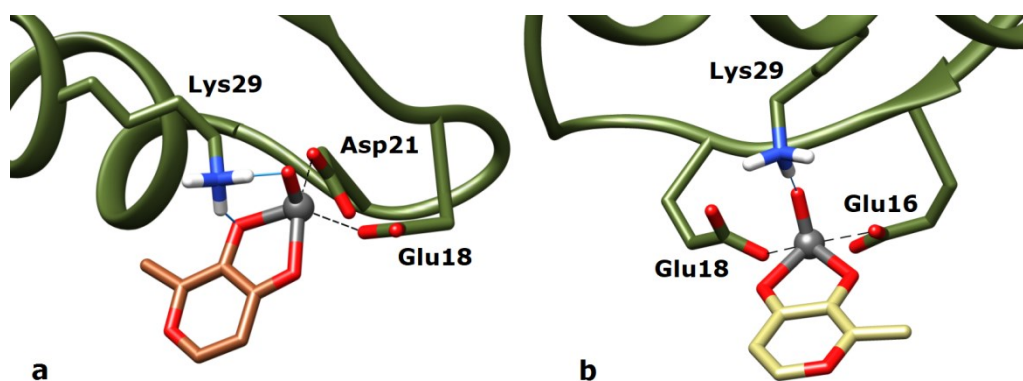


Figure 7. Most stable structures predicted by docking for the binding of VO(ma)⁺ to Ub: a) binding to site 1' with Glu18 and Asp21 of SPY-5-13-A-VO(ma)⁺; b) binding to site 1 with Glu16 and Glu18 of SPY-5-13-C-VO(ma)⁺. The hydrogen bonds are highlighted with the full blue lines.

Table 5. Docking solutions for the interaction of the mono-chelated VOL⁺ species with Ub.

Species	Site	Residues	V–O ^a	F_{\max} ^b	F_{mean} ^c	Pop. ^d	Rank. ^e
VO(ma) ⁺	1	Glu16, Glu18	2.256, 2.190	45.4	43.8	17%	II
	1'	Glu18, Asp21	2.029, 2.376	50.9	42.6	27%	I
	2	Glu24, Asp52	2.258, 2.295	42.2	39.6	63%	I
	2'	Glu51, Asp52	2.308, 2.278	39.9	38.7	36%	II
VO(koj) ⁺	1	Glu16, Glu18	2.313, 2.228	45.9	45.3	13%	II
	1'	Glu18, Asp21	1.916, 2.413	52.9	45.2	25%	I
	2	Glu24, Asp52	2.265, 2.311	42.4	40.6	44%	I
	2'	Glu51, Asp52	2.322, 2.148	41.5	39.5	21%	II
VO(acac) ⁺	1	Glu16, Glu18	2.300, 2.342	46.2	44.3	14%	I
	1'	Glu18, Asp21	2.382, 2.236	42.8	39.3	20%	II
	2	Glu24, Asp52	2.328, 2.353	38.2	37.2	88%	I
	2'	Glu51, Asp52	2.373, 2.373	36.3	34.9	12%	II

^a Distance between V and protein donors in Å. ^b GoldScore *Fitness* value obtained for the more stable pose of each *cluster* (F_{\max}). ^c Average value of GoldScore *Fitness* for each cluster (F_{mean}). ^d Population of the cluster (presented as percentage). ^e Ranking of the identified cluster.

Ternary system V^{IV}O²⁺/koj/Ub. Kojic acid is a ligand structurally similar to maltol and its complex with V^{IV}O²⁺ ion, [VO(kojato)₂], is a potential candidate in the treatment of diabetes.^{50, 57} The behavior of the system V^{IV}O²⁺/koj in aqueous solution is similar to that of V^{IV}O²⁺/ma and at pH 7.4 the major species is *cis*-[VO(koj)₂(H₂O)] (Scheme 1), as demonstrated by pH-potentiometric and spectroscopic measurements.⁵⁸

Anisotropic EPR spectra of the ternary system containing V^{IV}O²⁺, koj and Ub at pH 7.4 with molar ratios 1/2/1, 2/4/1 and 4/8/1 are reported in Figure S4. The results are comparable with those displayed by maltolate and the analysis of the spectra allows the identification of two adducts, VO(koj)₂(His-N) (III in Figure S4) and VO(koj)₂(Asp/Glu-COO) (IV). The A_z value for the species VO(koj)₂(His-N) ($165.0 \times 10^{-4} \text{ cm}^{-1}$) is comparable to that of the model complex *cis*-[VO(koj)₂(MeIm)] (II in Figure S4, $165.4 \times 10^{-4} \text{ cm}^{-1}$ ^{8f}), suggesting that protein coordinates the V^{IV}O²⁺ ion after the replacement of an equatorial water molecule with the imidazole-N of His68, while A_z of VO(koj)₂(Asp/Glu-COO) is ca. $168 \times 10^{-4} \text{ cm}^{-1}$. With increasing the ratio (VO(koj)₂/Ub), increases the intensity of the resonances due to VO(koj)₂(Asp/Glu-COO) and to the unbound complex *cis*-[VO(koj)₂(H₂O)] (I in Figure S4): this indicates that the number of Asp or Glu residues available for V binding is higher than those of His and that ubiquitin is not able to coordinate more than three equivalents of *cis*-VO(koj)₂ moiety. Therefore, the formula of the species formed can be indicated with 3[VO(koj)₂]-Ub. On the basis of the docking data obtained with maltol and considering the residue surface accessibility, His68, Glu16 or Glu18 and Asp21 could be the candidates for the V coordination.

ESI-MS spectra of the system with V^{IV}O²⁺, koj and ubiquitin were recorded at a protein concentration of 5 μM with varying the molar ratio between the complex and protein (3/1, 5/1 and 10/1). The deconvoluted spectra at ratio 5/1 and 10/1 show peaks attributable to the formation of the adducts [VO(koj)]-Ub and 2[VO(koj)]-Ub (Figure S5). The isotopic pattern for the peak observed

in the ESI-MS spectrum at $m/z = 1462.9$ and $z = 6$ was simulated with the molecular formula $C_{384}H_{635}N_{105}O_{123}SV$, that corresponds to the adduct $\{[VO(koj)]-Ub+H\}$ (Figure S6).

Anisotropic EPR spectra were also recorded with a molar ratio $V^{IV}O^{2+}/koj/Ub$ of 1/1/1 at different pH values to favor the binding of the mono-chelated complex $[VO(koj)(H_2O)_2]^+$ to the protein and eventually confirm the results obtained with ESI-MS (Figure S7). From an examination of Figure S7, it is possible to observe the species **I** identified as the mono-chelated complex $[VO(koj)(H_2O)_2]^+$, present both at pH 5.15 and 6.15 (traces b and d). The resonances indicated with **II** at pH 5.3 – when imidazole-N of His68 is still protonated – are attributed to the adduct with coordination $VO(koj)(Asp/Glu-COO)_2$, in which both the water ligands of $[VO(koj)(H_2O)_2]^+$ are replaced by carboxylate groups from aspartate or glutamate residues. These species are analogous to those observed with maltol (cfr. Figure S7 with Figure 6). Docking simulations (Table 5) were carried out with $VO(koj)^+$ moiety and indicate that, similarly to the system with maltolate, site **1'** with the binding of Glu18 and Asp 21 and **2** with Asp24 and Glu52 should be more stable than **1** (Glu16 and Glu18) and **2'** (Glu51 and Glu52) and account for the detection of the adduct $2[VO(koj)]-Ub$ by ESI-MS technique (Figure S5). The structure of the sites **1'** and **2** predicted by docking is represented in Figure 8.

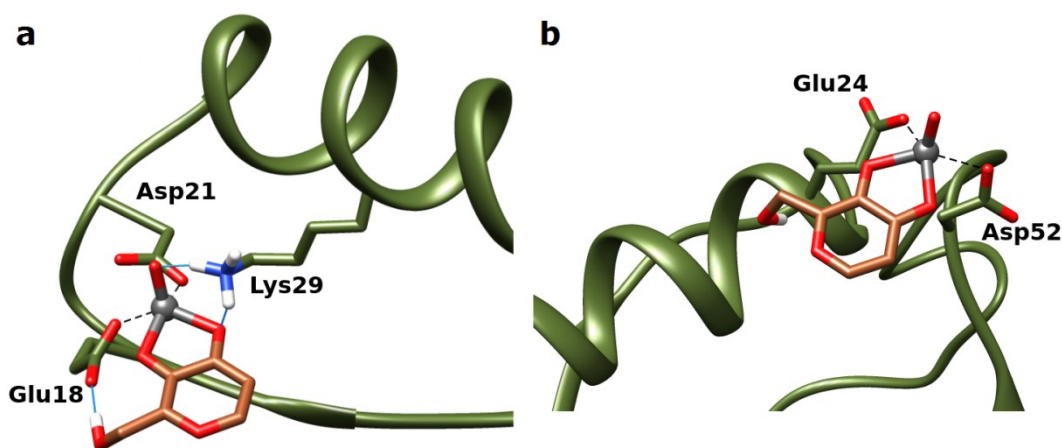


Figure 8. Most stable structures predicted by docking for the binding of $\text{VO}(\text{koj})^+$ to Ub: a) binding to site 1' with Glu18 and Asp21 of *SPY-5-13-A-VO(koj)*⁺; b) binding to site 2 with Glu24 and Asp52 of *SPY-5-13-C-VO(koj)*⁺. The hydrogen bonds are highlighted with the full blue lines.

Ternary system $\text{V}^{\text{IV}}\text{O}^{2+}/\text{acac}/\text{Ub}$. $[\text{VO}(\text{acac})_2]$ shows both antidiabetic and anticancer actions. It corrects the hyperglycemia and impairs hepatic glycolysis in streptozotocin-induced diabetic rats (STZ-rats) more potently than an inorganic V^{IV} salt, VOSO_4 ,⁵⁹ and recent results indicate that it could have a potential application in the treatment of pancreatic cancer.⁶⁰ In an aqueous solution, acetylacetonate forms with the $\text{V}^{\text{IV}}\text{O}^{2+}$ ion the species $[\text{VO}(\text{acac})(\text{H}_2\text{O})_2]^+$ and $[\text{VO}(\text{acac})_2]$,⁶¹ both of them with a square pyramidal geometry (see Scheme 1 for $[\text{VO}(\text{acac})_2]$).⁶² The stability constants indicate that at physiological pH and V concentration 1 mM the major species in solution is $[\text{VO}(\text{acac})_2]$, while at concentration 1 μM $[\text{VO}(\text{acac})(\text{H}_2\text{O})_2]^+$ predominates and the amount of $[\text{VO}(\text{acac})_2]$ is low.⁶¹ The consequence is that at the concentrations used with EPR spectroscopy (in the order of mM), the active binding with the formation of a coordination bond is precluded by the square pyramidal arrangement as demonstrated for other proteins,^{8b, 8d, 8h} this was observed also in the system with ubiquitin where the EPR spectra recorded at room temperature in a solution containing $[\text{VO}(\text{acac})_2]$ and Ub are exactly the same as those measured with $[\text{VO}(\text{acac})_2]$ only (Figure S8). In contrast, when the experiments are performed with the concentrations suitable for ESI-MS technique (in the range 10-50 μM), ubiquitin can interact with the two *cis* equatorial positions of $[\text{VO}(\text{acac})(\text{H}_2\text{O})_2]^+$ occupied by two weak water ligands.

The ESI-MS spectra on the system $[\text{VO}(\text{acac})_2]/\text{Ub}$ were recorded using an ubiquitin concentration of 5 μM and molar ratios 3/1, 5/1 and 10/1, as previously done for the systems with maltol and kojic acid. The deconvoluted spectrum at ratio 3/1 is represented in Figure 9 and shows the presence of the species $n[\text{VO}(\text{acac})_2]-\text{Ub}$, with $n = 1-3$. This means that ubiquitin binds three

fragments $\text{VO}(\text{acac})^+$. The experimental isotopic pattern for the peak corresponding to the most abundant adduct between $\text{VO}(\text{acac})^+$ and Ub was simulated and it was found to be coincident with the molecular formula $\text{C}_{383}\text{H}_{637}\text{N}_{105}\text{O}_{121}\text{SV}$, i.e. $[\text{VO}(\text{acac})]\text{-Ub}$ ($m/z = 1248.1$, $z = 7$, Figure S9).

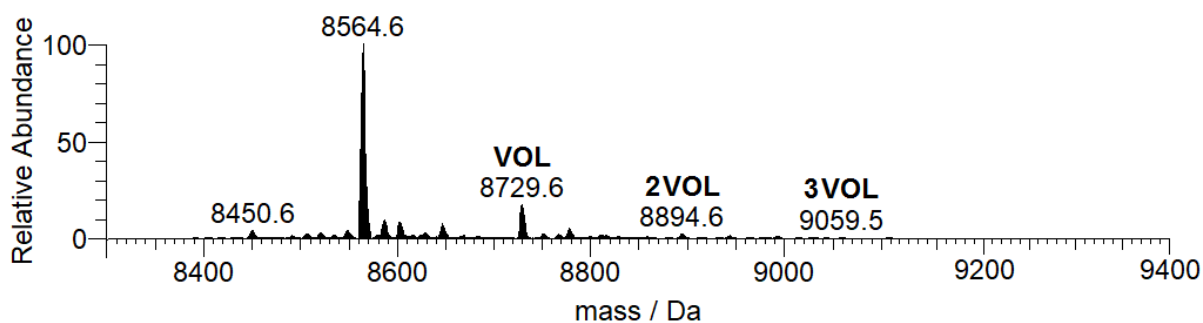


Figure 9. Deconvoluted ESI-MS spectrum recorded on the system containing $[\text{VO}(\text{acac})_2]$ and ubiquitin ($5 \mu\text{M}$) with molar ratio 3/1. With VOL the fragment $\text{VO}(\text{acac})^+$ that interacts with Ub is indicated.

To further support the conclusions drawn by EPR and ESI-MS about the adducts revealed, docking calculations were performed comparing the interaction between the mono- and bis-chelated species of acac with ubiquitin. In analogy with the previous calculations, for the $\text{VO}(\text{acac})^+$ moiety the regions with at least two potential coordinating residues were examined applying the GOLD rotamers libraries⁴⁵, while for $\text{VO}(\text{acac})_2$ the whole rigid protein was considered. For $\text{VO}(\text{acac})^+$, the results indicate the same four binding sites predicted for $\text{VO}(\text{ma})^+$ and $\text{VO}(\text{koj})^+$, i.e. the sites 1, 1', 2 and 2' (Table 5); however, it can be noted that the GoldScore values are slightly lower than those of maltolate and kojate due to the lower lipophilicity of the ligand, and there is an inversion of stability between the sites 1 and 1' with Glu16/Glu18 being favored compared to Glu18/Asp21 (Table 5 and Figure 10). The sites 1 and 2 can be related to the observation of $2[\text{VO}(\text{acac})]\text{-Ub}$

adduct by ESI-MS, while the third moiety $[\text{VO}(\text{acac})(\text{H}_2\text{O})_2]^+$ (see Figure 9) could be bound to a surface site of ubiquitin through secondary interactions favored during the desolvation process.

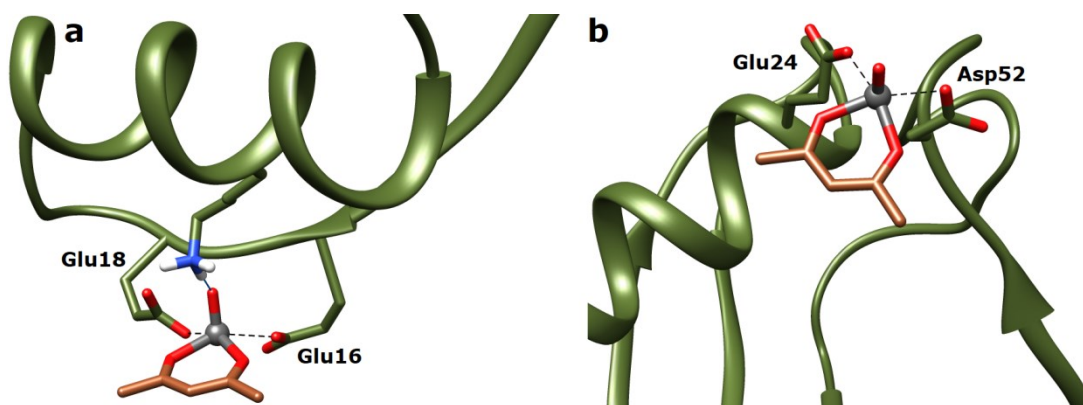


Figure 10. Most stable structures predicted by docking for the binding of $\text{VO}(\text{acac})^+$ to Ub: a) binding to site 1 with Glu16 and Glu18 of $\text{VO}(\text{acac})^+$; b) binding to site 2 with Glu24 and Asp52 of $\text{VO}(\text{acac})^+$. The hydrogen bonds are highlighted with the full blue lines.

For the prediction of the binding of the bis-chelated species $[\text{VO}(\text{acac})_2]$ to ubiquitin, we applied the modification of GoldScore in GOLD 5.2 software recently validated to predict the surface interactions of $\text{V}^{\text{IV}}\text{O}$ compounds with lysozyme.^{23c} In particular, we found that the scoring threshold that marks the transition from an *anisotropic* (strong interaction of $\text{V}^{\text{IV}}\text{O}$ species with the protein surface, which hinders the rotation of the complex in aqueous solution) to an *isotropic* EPR spectrum (weak interaction, with the complex free to rotate in solution) is 16-17 GoldScore units.^{23c} The docking calculations of this work show several clusters with comparable *Fitness* (Figure 11 and Table S1), indicating the absence of binding specificity; moreover, the GoldScore values ($F_{\text{max}} = 10.0$) are lower than the limit expected for a strong surface interaction and the weak binding is not able to block the rotation of $[\text{VO}(\text{acac})_2]$ longer than EPR timescale ($\sim 50 \text{ ns}$ ⁶³). For all the clusters,

the strongest interaction is a hydrogen bond between the V=O and side-chain NH/NH₂/NH₃⁺ groups of Arg42, Gln49, Lys6, His68, Arg54 and Arg72.

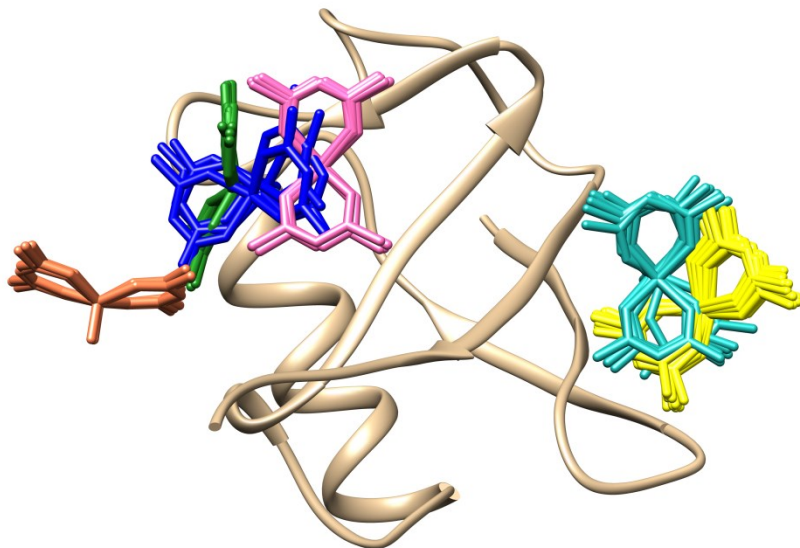


Figure 11. Cluster distribution for the interaction of [VO(acac)₂] with Ub. The six most stable clusters are represented with different colors.

Ternary system V^{IV}O²⁺/dhp/Ub. The antidiabetic and antitumor action of [VO(dhp)₂] has been proved in the literature,^{64, 65} and its biospeciation in the organism has been investigated for many years.^{3, 8b, 9a, 47, 66} The potentiometric and spectroscopic data indicate that, between pH 5 and 8, the bis-chelated species is the major one in aqueous solution. It is present as a mixture of [VO(dhp)₂], square pyramidal, and *cis*-[VO(dhp)₂(H₂O)], distorted octahedral, in equilibrium between each other (Scheme 1).^{31, 67}

Anisotropic EPR spectra of the ternary system containing V^{IV}O²⁺, dhp and Ub were recorded at pH 7.4 as a function of the ratio [VO(dhp)₂]/Ub (traces c-e in Figure 12). It can be immediately observed that the amount of the mixed adducts is very small since even when the ratio is 1/1 the resonances of the binary species *cis*-[VO(dhp)₂(H₂O)] (**Ia**) and [VO(dhp)₂] (**Ib**) are clearly

revealed. However, the broad absorption between 406 and 410 mT indicates the presence of a further species that may be the ternary $V^{IV}O$ -dhp-Ub adducts (**III** and **IV**). The value of A_z for **III** ($162.3 \times 10^{-4} \text{ cm}^{-1}$) is comparable with that of *cis*-[VO(dhp)₂(1-MeIm)] (**II**, $163.0 \times 10^{-4} \text{ cm}^{-1}$ ^{8b}), in which an equatorial water molecule of the *cis*-octahedral species is replaced by an imidazole nitrogen. This indicates the formation, in small amounts, of the mixed species VO(dhp)₂(His-N); the resonances of **IV** fall at higher magnetic field than **III** and this can be explained –according to the 'additivity relationship' ⁵⁴– with the presence in the fourth equatorial position of a carboxylate group from an Asp or Glu residue instead of a His-N in the adduct VO(dhp)₂(Asp/Glu-COO). On the basis of the docking results discussed in the previous sections, the residues candidate to bind VO(dhp)₂ moiety are Glu16, Glu18 and Asp21. When the ratio ($V^{IV}O$ complex)/Ub increases to 2 or 4 the spectrum coincides with that of the binary system.

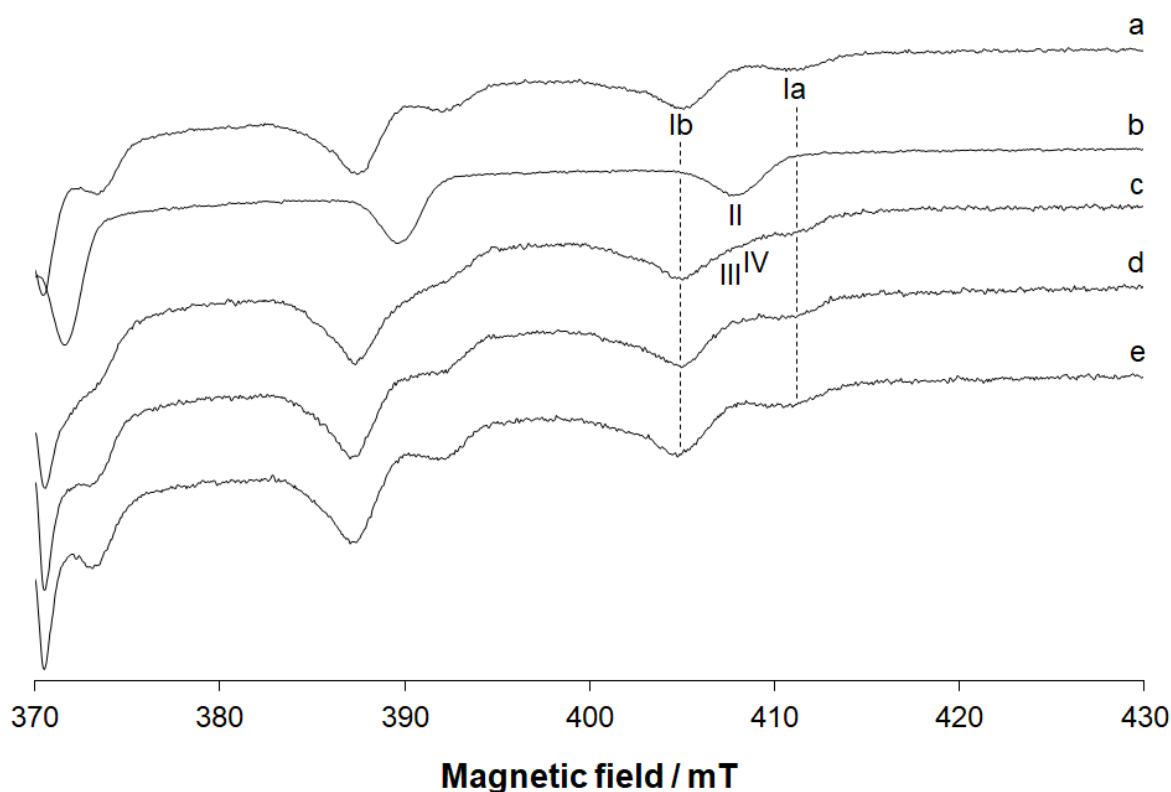


Figure 12. High field region of the EPR spectra recorded on frozen solutions (120 K) containing: a) $V^{IV}O^{2+}/dhp$ 1/2; b) $V^{IV}O^{2+}/dhp/1\text{-MeIm}$ 1/2/4; c) $V^{IV}O^{2+}/dhp/Ub$ 1/2/1; d) $V^{IV}O^{2+}/dhp/Ub$ 2/4/1; e)

$V^{IV}O^{2+}/dhp/Ub$ 4/8/1. $V^{IV}O^{2+}$ concentration was 1.0×10^{-3} M and pH was 7.4 in all the systems. The $M_1 = 7/2$ resonance of the adducts $VO(dhp)_2(His68)$ is indicated with **III** and of $VO(dhp)_2(Asp/Glu-COO)$ with **IV**. **Ia**, **Ib** and **II** indicate the $M_1 = 7/2$ resonances of *cis*- $[VO(dhp)_2(H_2O)]$, $[VO(dhp)_2]$ and *cis*- $[VO(dhp)_2(MeIm)]$, respectively. The resonances of the species present in the binary species, *cis*- $[VO(dhp)_2(H_2O)]$ and $[VO(dhp)_2]$, are also denoted with the dotted lines.

The ESI-MS spectra of the system $[VO(dhp)_2]/Ub$, recorded as a function of the molar ratio, are characterized by a very intense signal related to the free complex $[VO(dhp)_2+H]^+$ at $m/z = 344.0$. This reflects the low binding affinity of the binary species $V^{IV}O-dhp$ for ubiquitin, as demonstrated by the deconvoluted spectra reported in Figure S10. The only significant adducts that can be observed at the three ratios are $[VO(dhp)_2]-Ub$ (8907.7 Da) and $[VO(dhp)]-Ub$ (8768.6 Da), characterized by lower intensity in comparison with the peaks of the free protein. This suggests that the stability of the dhp adducts in solution, as indicated by EPR spectroscopy, is not as high as for *ma* and *koj*. The presence of $[VO(dhp)]-Ub$ is due to the low V concentration, which favors the hydrolysis of the system and the formation of $[VO(dhp)(H_2O)_2]^+$. To confirm the presence of $[VO(dhp)_2]-Ub$ in the ESI-MS spectra, the isotopic pattern of this peak was simulated (Figure S11): the agreement with the experimental result is obtained using the molecular formula $C_{392}H_{646}N_{107}O_{123}SV$ ($m/z = 1782.5$, $z = 5$).

Ternary system $V^{IV}O^{2+}/mim/Ub$. L-mimosine (*mim*) is an amino acid of plant origin with several biological properties, among which antitumoral, antiinflammatory, antiinfluenza, antiviral action.⁶⁸ The studies in the literature indicate that it blocks the cellular cycle in the G_1 phase.⁶⁸

Structurally, L-mimosine is a derivative of dhp, but two **alternative** coordination modes –with maltol-like (CO, O⁻) or amino acid-like (NH₂, COO⁻) **chelates** – are possible. EPR and potentiometric data suggests that L-mimosine forms with the V^{IV}O²⁺ ion at physiological pH a stable bis-chelated species with coordination mode similar to maltol and a *cis*-octahedral geometry, its composition being [VO(mim)₂(H₂O)]²⁻ with the carboxylic group of the amino acid in the deprotonated form (Scheme 1).⁶⁹

EPR spectra of the ternary system containing V^{IV}O²⁺, mim and Ub at pH 7.4 and ratio V^{IV}O/Ub of 1/1, 2/1 and 4/1 were reported in Figure S12. Three species were revealed: **III** and **IV** denote the two adducts VO(mim)₂(His-N) and VO(mim)₂(Asp/Glu-COO), analogous to those observed for dhp, and **I** the unbound binary species *cis*-[VO(mim)₂(H₂O)]²⁻. The binding between the complex and the protein takes place through the replacement of the equatorial water molecule with an imidazole of His 68 and with carboxylates of Asp or Glu residues, presumably Glu16, Glu18 and Asp21. The comparison between A_z of VO(mim)₂(His68) (**III** in trace c of Figure S12, $g_z = 1.948$ and $A_z = 165.1 \times 10^{-4} \text{ cm}^{-1}$) with *cis*-[VO(mim)₂(MeIm)]²⁻ (**II** in trace b of Figure S12, $g_z = 1.947$ and $A_z = 164.3 \times 10^{-4} \text{ cm}^{-1}$) confirms the His binding, while for VO(mim)₂(Asp/Glu-COO) a smaller value of g_z and a larger A_z are measured (**IV** in trace d of Figure S12, $g_z = 1.945$ and $A_z = 167.9 \times 10^{-4} \text{ cm}^{-1}$), as expected from the 'additivity relationship'⁵⁴. In comparison with the dhp system, the spectral signals of the adducts revealed with L-mimosine are much more intense suggesting that the coordination of mim could be stabilized by secondary interactions (hydrogen bonds and/or van der Waals contacts) between the NH₂ and COO⁻ groups, that do not participate to the metal coordination, and the protein.

The deconvoluted ESI-MS spectra of the system VO(mim)₂/Ub are shown in Figure S13. They are characterized by a low intensity of the peaks corresponding to the adducts {[VO(mim)]-Ub+H} and {[VO(mim)₂]-Ub+2H}, in which one fragment VO(mim) or VO(mim)₂²⁻ (with mass 264.0 and 461.0 Da, respectively) is bound to ubiquitin. Moreover, the peak of the adduct {[VO(mim)+VO(mim)₂]-Ub+3H} is observed. When the ratio is 10/1 the number of moieties

$\text{VO}(\text{mim})_2^{2-}$ bound to protein increases to 2, in agreement with what was detected by EPR spectroscopy. His68 and one residue among Glu16, Glu18 and Asp21 are the most plausible candidates for the V binding. The isotopic pattern for the peak observed in the spectrum at $m/z = 1505.3$ and $z = 6$ was simulated using the molecular formula $\text{C}_{394}\text{H}_{648}\text{N}_{109}\text{O}_{127}\text{SV}$ that corresponds to $\{[\text{VO}(\text{mim})_2]-\text{Ub}+2\text{H}\}$ and is represented in Figure S14.

Binding sites of Ub. Examining the results of this study, a series of coordination rules for the interaction of $\text{V}^{\text{IV}}\text{O}^{2+}$ ion and VOL_2 prodrugs with ubiquitin, and in general with proteins, can be inferred. For the bare oxidovanadium(IV) ion, the binding of at least a pair of amino acid **side chains**, particularly His-N or Asp/Glu-COO, is required. Secondary binding sites can involve the coordination of carbonyl-O of the backbone. From a geometric point of view, the β -carbon of the coordinating amino acids should be located approximately at 2.5 Å from vanadium, and donors should be able to bind $\text{V}^{\text{IV}}\text{O}^{2+}$ ion in an equatorial position. The binding sites, as demonstrated in this and previous published works ¹⁶, could be located on the surface as well as buried into the protein. The first coordination sphere of the metal, if is not completed by **side chain groups**, could be filled by water or hydroxide ligands depending on the pH and surrounding residues. Moreover, the metal coordination could be stabilized by hydrogen bonds between the oxido ligand of the $\text{V}^{\text{IV}}\text{O}^{2+}$ ion and amino acids as threonine, lysine, tyrosine, cysteine, arginine, etc. Hydrogen bond stabilization is, in some cases, the driving force for stabilizing structures with weak donors, such as in the case of the site **1** of Ub that shows a strong $\text{V}=\text{O}\cdots\text{H}_3\text{N}^+-\text{Lys}29$ interaction (see **Figure 2**).

The VOL_2 complexes interact with ubiquitin in three different modes: i) a bidentate ligand L^- is replaced by a couple of amino acid **side chain groups** to form $n[\text{VOL}]-\text{Ub}$ adducts, when n is the number of the potential sites of protein; ii) for *cis*- $[\text{VOL}_2(\text{H}_2\text{O})]$, a protein donor can replace the equatorial water molecule to give $n[\text{VOL}_2]-\text{Ub}$ mixed; iii) in the case of square pyramidal complexes $[\text{VOL}_2]$ the interaction is mainly non-covalent and takes place on the protein surface.

The $[\text{VOL}(\text{H}_2\text{O})_2]^+$ species, whose formation is favored by the hydrolysis of the system at low V concentration, have two *cis* accessible sites and can be bound by two neighboring residues if their β -carbons are within a distance ~ 2.5 Å from the metal and if these replace the two water molecules in the two adjacent free equatorial positions. In these situations the (Asp, Glu), (Asp, Asp) or (Glu, Glu) coordination can be enough, and the interaction of His occurs only if it is assisted by another coordinating residue. Hydrogen bond plays a fundamental role in the binding process: for example, the formation of strong interactions significantly favors the binding of $\text{VO}(\text{koj})^+$ to the **site 1** (Glu18, Asp21) (interaction of Lys29- NH_3^+ group with $\text{V}=\text{O}$ and coordinating CO, and carboxylate of Glu18 with the CH_2OH substituent in position 2 of kojate ring, Figure 8) over **site 2** (Glu24, Asp52) or **2'** (Glu51, Asp52) with about 10 GoldScore fitness units of difference (Table 5).

Finally, for the *cis*-octahedral species, it is possible to reinforce the previous conclusions on the possibility that aqua ligands are exchanged, forming adducts with not hindered and solvent exposed amino acid side chains, for example those belonging to Asp/Glu or His residues.^{8m} In general, coordination of the metal through carboxylate containing side chains only occurs in the absence of accessible histidines (lysozyme, for example, for which the unique His residue, His15, is not exposed enough^{23a}) or if strong hydrogen bonds are formed reverting the general of stability order $\text{His-N} > \text{Asp/Glu-COO}$. In this study, the affinity of *cis*- $\text{VO}(\text{ma})_2$ for His68 is much lower than for Glu18 and Asp21 due to the contact $\text{V}=\text{O}\cdots\text{H}_3\text{N}^+-\text{Lys29}$ interaction (Figure 4 and Table 3).

The relative stability of the adducts $n[\text{VOL}_2]-\text{Ub}$ and $n[\text{VOL}]-\text{Ub}$ can be related mainly to the thermodynamic stability of the bis-chelated VOL_2 complex; in particular, when the ligand L has intermediate strength (for example, ma, koj and acac) the formation of VOL^+ moiety is favored at the low concentrations used in the mass spectrometry experiments (some μM), while when L is stronger (dhp and mim) VOL_2 survives in part in aqueous solution and both the fragments VOL^+ and VOL_2 are revealed by ESI-MS (see Figures S10 and S13).

A general overview of the Ub binding sites is given in **Figure 13** in which the coordinating residues and **the position of sites 1, 1', 2 and 2'** are explicitly shown.

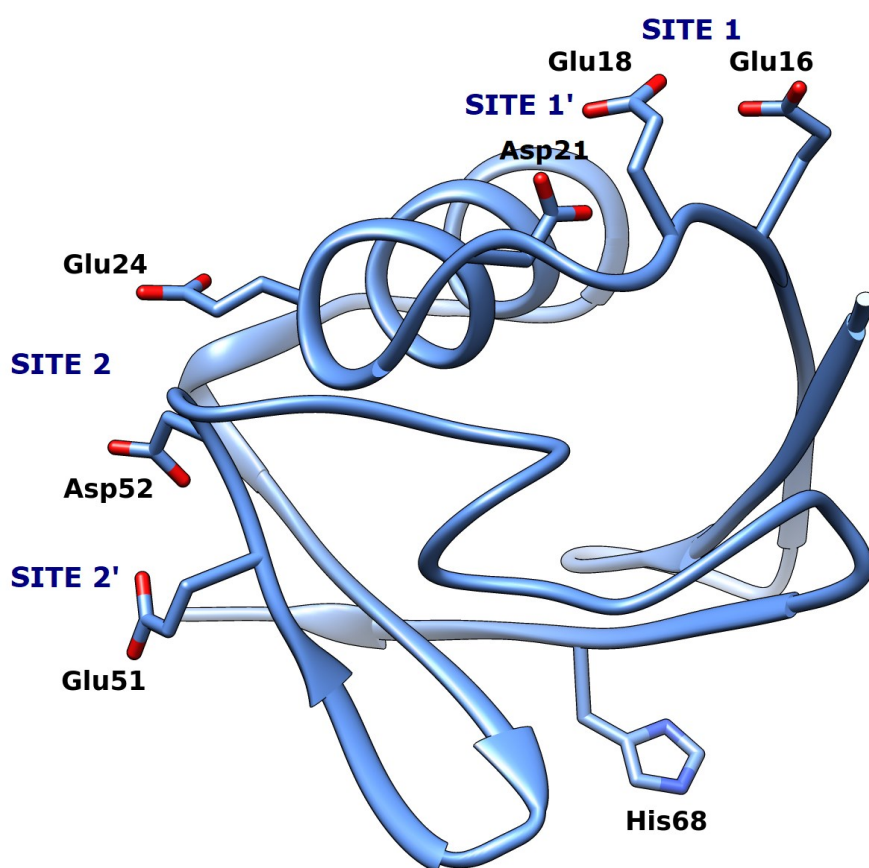


Figure 13. Ubiquitin view in ribbon style with the coordinating residues found in this work shown in stick representation. The sites 1, 1', 2 and 2' are also indicated.

Conclusions

The interaction of $V^{IV}O^{2+}$ ion and some of its bis-chelated pharmacologically active complexes formed by pyranones (maltol, kojic acid), pyridinones (dhp and L-mimosine) and acetylacetonone with ubiquitin was characterized through the combined application of spectroscopic (EPR), spectrometric (ESI-MS) and computational (docking and DFT methods) techniques. Since the complexes studied exhibit a wide range of chemical features such as thermodynamic stability,

geometry, charge and H-bond donor/acceptor groups, the results obtained allowed us to establish which factors lead to the formation of stable adducts.

When considering the binary system $V^{IV}O^{2+}/Ub$, the docking approach allowed us to identify the residues able to coordinate the metal: His68, the only one histidine of ubiquitin, and residues of Glu16, Glu18, Asp21, Glu24, Asp51 and Glu52; in contrast, Met1 – which binds Pt species – does not seem to take part in the coordination. This confirms the results in the literature which suggest that His, Asp and Glu residues have the highest affinity for V^{IV} under physiological conditions. With $V^{IV}O^{2+}$ ion the most stable site is based on the contemporaneous coordination of Glu16 and Glu18 (site 1).

With the $V^{IV}OL_2$ complexes the interaction depends on their geometry at pH 7.4 and on the V concentration used. Three cases were found: i) when the concentration is around some mM and the *cis*-octahedral $VOL_2(H_2O)$ species (formed in our systems by ma, koj, dhp, and mim) are prevailing, they form adducts with composition $VOL_2(Asp/Glu-COO)$ (more stable) and $VOL_2(His-N)$ (less stable); ii) when the concentration is around some mM and the square pyramidal species VOL_2 (formed in this study by acac) exist in solution, they interact non-covalently with the protein surface; iii) when the concentration approaches μM , i.e. that found when a potential V drug is orally administered, the hydrolysis favors the formation of $VOL(H_2O)_2^+$ and the adducts $n[VOL]-Protein$ can be formed, where n depends on the number of available sites. Docking allows predicting the sites with at least two amino acid side chains able to bind contemporaneously two equatorial positions of the $V^{IV}O^{2+}$ ion: for ubiquitin they are the not-independent sites 1 and 1' with (Glu16, Glu18) and (Glu18, Asp 21), and 2 and 2' with (Asp24, Glu52) and (Glu51, Glu52), shown in Figure 13.

The results obtained here could open new prospects to study the interaction of metal complexes with proteins. The data demonstrate that the $V^{IV}O$ binding is a manifold and complicated process which depends on the specific conformation of the protein, on the stability and geometry of the complexes and on the capability of the organic ligand to establish secondary interactions with the

proteic scaffold. In particular, once a specific site in a protein has been ascertained by docking, it could be possible to establish which metal species better interacts with such a site depending on its structure and possibility to form H-bonds or van der Waals contacts; in this way the best candidate for the interaction could be selected. On the other hand, if the interaction would not be desirable, the metal adduct which less effectively interacts with the protein site could be predicted. The adducts formed can influence the transport and uptake in the target cells of the pharmacologically active V compounds and the knowledge of their structures and stability could be exploited for a rational design of new V potential drugs.

Supporting Information

The Supporting Information is available free of charge on the ACS Publications website at DOI: 10.1021/acs.inorgchem.xxxxxxx. Table with docking results for the interaction of [VO(acac)₂] with ubiquitin (Table S1), figures with the deconvoluted ESI-MS spectra recorded in the systems with ubiquitin, VO(koj)₂/Ub, VO(dhp)₂/Ub and V^{IV}O²⁺/mim/Ub (Figures S1, S5, S10, and S13), figures with the calculated isotopic pattern for the adducts [VO(ma)]-Ub, [V^VO₂]-Ub, {[VO(koj)]-Ub+H}, [VO(acac)]-Ub, [VO(dhp)₂]-Ub, and {[VO(mim)₂]-Ub+2H} (Figures S2, S3, S6, S9, S11, and S14), figures with EPR spectra recorded in the systems V^{IV}O²⁺/koj/Ub, V^{IV}O²⁺/acac/Ub and V^{IV}O²⁺/mim/Ub (Figures S4, S7, S8 and S12).

Author Information

Corresponding Authors

* For D.S.: phone, +39 079 2841207; E-mail, daniele.sanna@cnr.it

* For E.G.: phone, +39 079 229487; E-mail, garribba@uniss.it

ORCID

Valeria Ugone: 0000-0002-2830-3869

Daniele Sanna: 0000-0001-9299-0141

Giuseppe Sciortino: 0000-0001-9657-1788

Jean-Didier Maréchal: 0000-0002-8344-9043

Eugenio Garribba: 0000-0002-7229-5966

Notes

The authors declare no competing financial interest.

Acknowledgments

This work was supported by the Spanish grant CTQ2017-87889-P and Generalitat de Catalunya 2017SGR1323, COST Action CM1306, Fondazione di Sardegna (project FDS15Garribba) and FFABR 2017 “Fondo per il finanziamento delle attività base di ricerca”. G.S. is also grateful to the Universitat Autònoma de Barcelona for the support to his Ph.D. The authors thank also Prof. Agustí Lledos (Universitat Autònoma de Barcelona) for his valuable suggestions.

References

- (1) Costa Pessoa, J.; Etcheverry, S.; Gambino, D. Vanadium compounds in medicine. *Coord. Chem. Rev.* **2015**, *301-302*, 24-48.
- (2) Rehder, D. Perspectives for vanadium in health issues. *Future Med. Chem.* **2016**, *8*, 325-338.
- (3) Jakusch, T.; Kiss, T. In vitro study of the antidiabetic behavior of vanadium compounds. *Coord. Chem. Rev.* **2017**, *351*, 118-126.
- (4) Levina, A.; Crans, D. C.; Lay, P. A. Speciation of metal drugs, supplements and toxins in media and bodily fluids controls *in vitro* activities. *Coord. Chem. Rev.* **2017**, *352*, 473-498.
- (5) Crans, D. C.; Henry, L.; Cardiff, G.; Posner, B. I. Developing Vanadium as Antidiabetic and Anticancer Drugs: A Clinical and Historical Perspective In *Essential Metals in Medicine: Therapeutic Use and Toxicity of Metal Ions in the Clinic*; Carver, P. L., Ed.; De Gruyter GmbH: Berlin, 2019; Vol. 19, pp 203-230.
- (6) Costa Pessoa, J.; Garribba, E.; Santos, M. F. A.; Santos-Silva, T. Vanadium and proteins: uptake, transport, structure, activity and function. *Coord. Chem. Rev.* **2015**, *301-302*, 49-86.
- (7) Sanna, D.; Ugone, V.; Micera, G.; Buglyo, P.; Biro, L.; Garribba, E. Speciation in human blood of Metvan, a vanadium based potential anti-tumor drug. *Dalton Trans.* **2017**, *46*, 8950-8967.
- (8) (a) Sanna, D.; Micera, G.; Garribba, E. On the Transport of Vanadium in Blood Serum. *Inorg. Chem.* **2009**, *48*, 5747-5757. (b) Sanna, D.; Micera, G.; Garribba, E. New Developments in the Comprehension of the Biotransformation and Transport of Insulin-Enhancing Vanadium Compounds in the Blood Serum. *Inorg. Chem.* **2010**, *49*, 174-187. (c) Sanna, D.; Buglyó, P.; Micera, G.; Garribba, E. A quantitative study of the biotransformation of insulin-enhancing VO²⁺ compounds. *J. Biol. Inorg. Chem.* **2010**, *15*, 825-839. (d) Sanna, D.; Micera, G.; Garribba, E. Interaction of VO²⁺ Ion and Some Insulin-Enhancing Compounds with Immunoglobulin G. *Inorg. Chem.* **2011**, *50*, 3717-3728. (e) Sanna, D.; Biro, L.; Buglyo, P.; Micera, G.; Garribba, E. Biotransformation of BMOV in the presence of blood serum proteins. *Metallomics* **2012**, *4*, 33-36. (f) Sanna, D.; Bíró, L.; Buglyó, P.; Micera, G.; Garribba, E. Transport of the anti-diabetic VO²⁺ complexes formed by pyrone derivatives in the blood serum. *J. Inorg. Biochem.* **2012**, *115*, 87-99. (g) Sanna, D.; Ugone, V.; Micera, G.; Garribba, E. Temperature and solvent structure dependence of VO²⁺ complexes of pyridine-N-oxide derivatives and their interaction with human serum transferrin. *Dalton Trans.* **2012**, *41*, 7304-7318. (h) Sanna, D.; Micera, G.; Garribba, E. Interaction of Insulin-Enhancing Vanadium Compounds with Human Serum holo-Transferrin. *Inorg. Chem.* **2013**, *52*, 11975-11985. (i) Koleša-Dobravec, T.; Lodyga-Chruscinska, E.; Symonowicz, M.; Sanna,

D.; Meden, A.; Perdih, F.; Garribba, E. Synthesis and characterization of $V^{IV}O$ complexes of picolinate and pyrazine derivatives. Behavior in the solid state and aqueous solution and biotransformation in the presence of blood plasma proteins. *Inorg. Chem.* **2014**, *53*, 7960-7976. (j) Sanna, D.; Fabbri, D.; Serra, M.; Buglyó, P.; Bíró, L.; Ugone, V.; Micera, G.; Garribba, E. Characterization and biotransformation in the plasma and red blood cells of $V^{IV}O^{2+}$ complexes formed by ceftriaxone. *J. Inorg. Biochem.* **2015**, *147*, 71-84. (k) Sanna, D.; Ugone, V.; Pisano, L.; Serra, M.; Micera, G.; Garribba, E. Behavior of the potential antitumor $V^{IV}O$ complexes formed by flavonoid ligands. 2. Characterization of sulfonate derivatives of quercetin and morin, interaction with the bioligands of the plasma and preliminary biotransformation studies. *J. Inorg. Biochem.* **2015**, *153*, 167-177. (l) Sanna, D.; Ugone, V.; Serra, M.; Garribba, E. Speciation of potential anti-diabetic vanadium complexes in real serum samples. *J. Inorg. Biochem.* **2017**, *173*, 52-65. (m) Sanna, D.; Ugone, V.; Sciortino, G.; Buglyó, P.; Bihari, Z.; Parajdi-Losoncz, P. L.; Garribba, E. $V^{IV}O$ complexes with antibacterial quinolone ligands and their interaction with serum proteins. *Dalton Trans.* **2018**, *47*, 2164-2182. (n) Sanna, D.; Palomba, J.; Lubinu, G.; Buglyó, P.; Nagy, S.; Perdih, F.; Garribba, E. Role of Ligands in the Uptake and Reduction of V(V) Complexes in Red Blood Cells. *J. Med. Chem.* **2019**, *62*, 654-664.

(9) (a) Jakusch, T.; Hollender, D.; Enyedy, E. A.; Gonzalez, C. S.; Montes-Bayon, M.; Sanz-Medel, A.; Costa Pessoa, J.; Tomaz, I.; Kiss, T. Biospeciation of various antidiabetic $V^{IV}O$ compounds in serum. *Dalton Trans.* **2009**, 2428-2437. (b) Correia, I.; Jakusch, T.; Cobbinna, E.; Mehtab, S.; Tomaz, I.; Nagy, N. V.; Rockenbauer, A.; Costa Pessoa, J.; Kiss, T. Evaluation of the binding of oxovanadium(IV) to human serum albumin. *Dalton Trans.* **2012**, *41*, 6477-6487. (c) Gonçalves, G.; Tomaz, A. I.; Correia, I.; Veiros, L. F.; Castro, M. M. C. A.; Avecilla, F.; Palacio, L.; Maestro, M.; Kiss, T.; Jakusch, T.; Garcia, M. H. V.; Costa Pessoa, J. A novel $V^{IV}O$ -pyrimidinone complex: synthesis, solution speciation and human serum protein binding. *Dalton Trans.* **2013**, *42*, 11841-11861. (d) Justino, G. C.; Garribba, E.; Costa Pessoa, J. Binding of $V^{IV}O^{2+}$ to the Fe binding sites of human serum transferrin. A theoretical study. *J. Biol. Inorg. Chem.* **2013**, *18*, 803-813. (e) Mehtab, S.; Gonçalves, G.; Roy, S.; Tomaz, A. I.; Santos-Silva, T.; Santos, M. F. A.; Romão, M. J.; Jakusch, T.; Kiss, T.; Costa Pessoa, J. Interaction of vanadium(IV) with human serum apo-transferrin. *J. Inorg. Biochem.* **2013**, *121*, 187-195. (f) Costa Pessoa, J.; Gonçalves, G.; Roy, S.; Correia, I.; Mehtab, S.; Santos, M. F. A.; Santos-Silva, T. New insights on vanadium binding to human serum transferrin. *Inorg. Chim. Acta* **2014**, *420*, 60-68. (g) Santos, M. F. A.; Correia, I.; Oliveira, A. R.; Garribba, E.; Costa Pessoa, J.; Santos-Silva, T. Vanadium Complexes as Prospective Therapeutics: Structural Characterization of a V^{IV} Lysozyme Adduct. *Eur. J. Inorg. Chem.* **2014**, 3293-3297. (h) Costa Pessoa, J. Thirty years through vanadium chemistry. *J. Inorg.*

- Biochem.* **2015**, 4-24. (i) Correia, I.; Chorna, I.; Cavaco, I.; Roy, S.; Kuznetsov, M. L.; Ribeiro, N.; Justino, G.; Marques, F.; Santos-Silva, T.; Santos, M. F. A.; Santos, H. M.; Capelo, J. L.; Douth, J.; Costa Pessoa, J. Interaction of $[V^{IV}O(acac)_2]$ with human serum transferrin and albumin. *Chem. Asian J.* **2017**, *12*, 2062-2084. (j) Azevedo, C. G.; Correia, I.; dos Santos, M. M. C.; Santos, M. F. A.; Santos-Silva, T.; Douth, J.; Fernandes, L.; Santos, H. M.; Capelo, J. L.; Costa Pessoa, J. Binding of vanadium to human serum transferrin - voltammetric and spectrometric studies. *J. Inorg. Biochem.* **2018**, *180*, 211-221.
- (10) (a) Thompson, K., H.; Liboiron Barry, D.; Hanson Graeme, R.; Orvig, C. In Vivo Coordination Chemistry and Biocalization of Bis(ligand)oxovanadium(IV) Complexes for Diabetes Treatment. In *Medicinal Inorganic Chemistry*; Sessler, J. L., Doctrow, S. R., McMurry, T. J., Lippard, S. J., Ed.; American Chemical Society: Washington DC, 2005; Vol. 903, pp 384-399. (b) Liboiron, B. D.; Thompson, K. H.; Hanson, G. R.; Lam, E.; Aebischer, N.; Orvig, C. New Insights into the Interactions of Serum Proteins with Bis(maltolato)oxovanadium(IV): Transport and Biotransformation of Insulin-Enhancing Vanadium Pharmaceuticals. *J. Am. Chem. Soc.* **2005**, *127*, 5104-5115.
- (11) Willsky, G. R.; Goldfine, A. B.; Kostyniak, P. J.; McNeill, J. H.; Yang, L. Q.; Khan, H. R.; Crans, D. C. Effect of vanadium(IV) compounds in the treatment of diabetes: in vivo and in vitro studies with vanadyl sulfate and bis(maltolato)oxovanadium(IV). *J. Inorg. Biochem.* **2001**, *85*, 33-42.
- (12) Crans, D. C.; Smee, J. J.; Gaidamauskas, E.; Yang, L. The Chemistry and Biochemistry of Vanadium and the Biological Activities Exerted by Vanadium Compounds. *Chem. Rev.* **2004**, *104*, 849-902.
- (13) Rehder, D. *Bioinorganic Vanadium Chemistry*. John Wiley & Sons Ltd.: Chichester, 2008.
- (14) (a) Bijelic, A.; Aureliano, M.; Rompel, A. The antibacterial activity of polyoxometalates: structures, antibiotic effects and future perspectives. *Chem. Commun.* **2018**, *54*, 1153-1169. (b) Bijelic, A.; Aureliano, M.; Rompel, A. Polyoxometalates as potential next-generation metallodrugs in the combat against cancer. *Angew. Chem., Int. Ed.* **2018**, *57*, 2-22.
- (15) (a) Ramos, S.; Moura, J. J. G.; Aureliano, M. Recent advances into vanadyl, vanadate and decavanadate interactions with actin. *Metallomics* **2012**, *4*, 16-22. (b) Aureliano, M.; Ohlin, C. A. Decavanadate in vitro and in vivo effects: facts and opinions. *J. Inorg. Biochem.* **2014**, *137*, 123-130.
- (16) Sciortino, G.; Garribba, E.; Maréchal, J.-D. Validation and Applications of Protein-Ligand Docking Approaches Improved for Metalloligands with Multiple Vacant Sites. *Inorg. Chem.* **2019**, *58*, 294-306.

- (17) Chasteen, D. N. Vanadium-Protein Interactions. In *Met. Ions Biol. Syst.*; Sigel, H., Sigel, A., Ed.; Marcel Dekker: New York, 1995; Vol. 31, pp 231-247.
- (18) (a) Butler, A.; Carter, J. N.; Simpson, M. T. Vanadium in Proteins and Enzyme. In *Handbook on Metalloproteins*; Bertini, I., Sigel, A., Sigel, H., Ed.; Marcel Dekker: New York, 2001; pp 153-179. (b) Mukherjee, B.; Halder, S.; Ghosh, M. K.; Manasadeepa, R. Vanadium Ions and Proteins, Distribution, Metabolism, and Biological Significance. In *Encyclopedia of Metalloproteins*; Kretsinger, R. H., Uversky, V. N., Permyakov, E. A., Ed.; Springer New York: New York, 2013; pp 2306-2316.
- (19) Rittle, J.; Field, M. J.; Green, M. T.; Tezcan, F. A. An efficient, step-economical strategy for the design of functional metalloproteins. *Nature Chem.* **2019**, *11*, 434-441.
- (20) Hartinger, C. G.; Groessl, M.; Meier, S. M.; Casini, A.; Dyson, P. J. Application of mass spectrometric techniques to delineate the modes-of-action of anticancer metallodrugs. *Chem. Soc. Rev.* **2013**, *42*, 6186-99.
- (21) Wenzel, M.; Casini, A. Mass spectrometry as a powerful tool to study therapeutic metallodrugs speciation mechanisms: Current frontiers and perspectives. *Coord. Chem. Rev.* **2017**, *352*, 432-460.
- (22) (a) Gibson, D.; Costello, C. A mass spectral study of the binding of the anticancer drug cisplatin to ubiquitin. *Eur. J. Mass Spectrom.* **1999**, *5*, 501-510. (b) Peleg-Shulman, T.; Najajreh, Y.; Gibson, D. Interactions of cisplatin and transplatin with proteins: Comparison of binding kinetics, binding sites and reactivity of the Pt-protein adducts of cisplatin and transplatin towards biological nucleophiles. *J. Inorg. Biochem.* **2002**, *91*, 306-311. (c) Najajreh, Y.; Peleg-Shulman, T.; Moshel, O.; Farrell, N.; Gibson, D. Ligand effects on the binding of *cis*- and *trans*-[PtCl₂Am₁Am₂] to proteins. *JBIC, J. Biol. Inorg. Chem.* **2003**, *8*, 167-175. (d) Hartinger, C. G.; Tsybin, Y. O.; Fuchser, J.; Dyson, P. J. Characterization of Platinum Anticancer Drug Protein-Binding Sites Using a Top-Down Mass Spectrometric Approach. *Inorg. Chem.* **2008**, *47*, 17-19. (e) Williams, J. P.; Phillips, H. I. A.; Campuzano, I.; Sadler, P. J. Shape changes induced by N-terminal platination of ubiquitin by cisplatin. *J. Am. Soc. Mass Spectrom.* **2010**, *21*, 1097-1106.
- (23) (a) Sciortino, G.; Sanna, D.; Ugone, V.; Micera, G.; Lledós, A.; Maréchal, J.-D.; Garribba, E. Elucidation of Binding Site and Chiral Specificity of Oxidovanadium Drugs with Lysozyme through Theoretical Calculations. *Inorg. Chem.* **2017**, *56*, 12938-12951. (b) Sciortino, G.; Rodríguez-Guerra Pedregal, J.; Lledós, A.; Garribba, E.; Maréchal, J.-D. Prediction of the interaction of metallic moieties with proteins: an update for protein-ligand docking techniques. *J. Comput. Chem.* **2018**, *39*, 42-51. (c) Sciortino, G.; Sanna, D.; Ugone, V.; Lledós, A.; Maréchal, J.-

D.; Garribba, E. Decoding Surface Interaction of V^{IV}O Metallodrug Candidates with Lysozyme. *Inorg. Chem.* **2018**, *57*, 4456-4469.

(24) Rehder, D. Vanadium. Its Role for Humans. In *Interrelations between Essential Metal Ions and Human Diseases*; Sigel, A., Sigel, H., Sigel, R. K. O., Ed.; Springer Science+Business Media: Dordrecht, 2013; pp 139-169.

(25) Crans, D., C.; Yang, L.; Haase, A.; Yang, X. Health Benefits of Vanadium and Its Potential as an Anticancer Agent. In *Metallo-Drugs: Development and Action of Anticancer Agents*; Sigel, A., Sigel, H., Freisinger, E., Sigel, R. K. O., Ed.; De Gruyter GmbH: Berlin, 2018; Vol. 18, pp 251-280.

(26) Hartinger, C. G.; Ang, W. H.; Casini, A.; Messori, L.; Keppler, B. K.; Dyson, P. J. Mass spectrometric analysis of ubiquitin–platinum interactions of leading anticancer drugs: MALDI versus ESI. *J. Anal. At. Spectrom.* **2007**, *22*, 960-967.

(27) Hartinger, C. G.; Casini, A.; Duhot, C.; Tsybin, Y. O.; Messori, L.; Dyson, P. J. Stability of an organometallic ruthenium-ubiquitin adduct in the presence of glutathione: relevance to antitumour activity. *J. Inorg. Biochem.* **2008**, *102*, 2136-41.

(28) Nagypál, I.; Fábíán, I. NMR relaxation studies in solution of transition metal complexes. V. Proton exchange reactions in aqueous solutions of VO²⁺-oxalic acid, -malonic acid systems. *Inorg. Chim. Acta* **1982**, *61*, 109-113.

(29) Orvig, C.; Caravan, P.; Gelmini, L.; Glover, N.; Herring, F. G.; Li, H.; McNeill, J. H.; Rettig, S. J.; Setyawati, I. A. Reaction chemistry of BMOV, bis(maltolato)oxovanadium(IV), a potent insulin mimetic agent. *J. Am. Chem. Soc.* **1995**, *117*, 12759-12770.

(30) Levina, A.; McLeod, A. I.; Lay, P. A. Vanadium Speciation by XANES Spectroscopy: A Three-Dimensional Approach. *Chemistry–A European Journal* **2014**, *20*, 12056-12060.

(31) Buglyo, P.; Kiss, T.; Kiss, E.; Sanna, D.; Garribba, E.; Micera, G. Interaction between the low molecular mass components of blood serum and the VO(IV)-DHP system (DHP = 1,2-dimethyl-3-hydroxy-4(1H)-pyridinone). *J. Chem. Soc., Dalton Trans.* **2002**, 2275-2282.

(32) Sanna, D.; Garribba, E.; Micera, G. Interaction of VO²⁺ ion with human serum transferrin and albumin. *J. Inorg. Biochem.* **2009**, *103*, 648-655.

(33) Frisch, M. J.; Trucks, G. W.; Schlegel, H. B.; Scuseria, G. E.; Robb, M. A.; Cheeseman, J. R.; Scalmani, G.; Barone, V.; Mennucci, B.; Petersson, G. A.; Nakatsuji, H.; Caricato, M. L., X.; Hratchian, H. P.; Izmaylov, A. F.; Bloino, J.; Zheng, G.; Sonnenberg, J. L.; Hada, M.; Ehara, M.; Toyota, K.; Fukuda, R.; Hasegawa, J.; Ishida, M.; Nakajima, T.; Honda, Y.; Kitao, O.; Nakai, H.; Vreven, T.; Montgomery, J. A., Jr.; Peralta, J. E.; Ogliaro, F.; Bearpark, M.; Heyd, J. J.; Brothers, E.; Kudin, K. N.; Staroverov, V. N.; Keith, T.; Kobayashi, R.; Normand, J.; Raghavachari, K.;

Rendell, A.; Burant, J. C.; Iyengar, S. S.; Tomasi, J.; Cossi, M.; Rega, N.; Millam, J. M.; Klene, M.; Knox, J. E.; Cross, J. B.; Bakken, V.; Adamo, C. J., J.; Gomperts, R.; Stratmann, R. E.; Yazyev, O.; Austin, A. J.; Cammi, R.; Pomelli, C.; Ochterski, J. W.; Martin, R. L.; Morokuma, K.; Zakrzewski, V. G.; Voth, G. A.; Salvador, P.; Dannenberg, J. J.; Dapprich, S.; Daniels, A. D.; Farkas, Ö.; Foresman, J. B.; Ortiz, J. V.; Cioslowski, J.; Fox, D. J. *Gaussian 09, revision D.01*. Gaussian, Inc.: Wallingford, CT, 2010.

(34) Marenich, A. V.; Cramer, C. J.; Truhlar, D. G. Universal Solvation Model Based on Solute Electron Density and on a Continuum Model of the Solvent Defined by the Bulk Dielectric Constant and Atomic Surface Tensions. *J. Phys. Chem. B* **2009**, *113*, 6378-6396.

(35) (a) Bühl, M.; Kabrede, H. Geometries of Transition-Metal Complexes from Density-Functional Theory. *J. Chem. Theory Comput.* **2006**, *2*, 1282-1290. (b) Bühl, M.; Reimann, C.; Pantazis, D. A.; Bredow, T.; Neese, F. Geometries of Third-Row Transition-Metal Complexes from Density-Functional Theory. *J. Chem. Theory Comput.* **2008**, *4*, 1449-1459.

(36) Micera, G.; Garribba, E. The effect of the functional, basis set, and solvent in the simulation of the geometry and spectroscopic properties of $V^{IV}O^{2+}$ complexes. Chemical and biological applications. *Int. J. Quantum Chem.* **2012**, *112*, 2486-2498.

(37) (a) Micera, G.; Pecoraro, V. L.; Garribba, E. Assessing the Dependence of ^{51}V A_z Value on the Aromatic Ring Orientation of $V^{IV}O^{2+}$ Pyridine Complexes. *Inorg. Chem.* **2009**, *48*, 5790-5796.

(b) Micera, G.; Garribba, E. Application of DFT Methods in the Study of $V^{IV}O^{2+}$ -Peptide Interactions. *Eur. J. Inorg. Chem.* **2010**, 4697-4710. (c) Sanna, D.; Várnagy, K.; Timári, S.; Micera, G.; Garribba, E. VO^{2+} Complexation by Bioligands Showing Keto-Enol Tautomerism: A Potentiometric, Spectroscopic, and Computational Study. *Inorg. Chem.* **2011**, *50*, 10328-10341. (d) Micera, G.; Garribba, E. The Effect of Trigonal Bipyramidal Distortion of Pentacoordinate $V^{IV}O^{2+}$ Species on their Structural, Electronic and Spectroscopic Parameters. *Eur. J. Inorg. Chem.* **2011**, 3768-3780.

(e) Sanna, D.; Pecoraro, V.; Micera, G.; Garribba, E. Application of DFT methods to the study of the coordination environment of the VO^{2+} ion in V proteins. *J. Biol. Inorg. Chem.* **2012**, *17*, 773-790.

(f) Pisano, L.; Várnagy, K.; Timári, S.; Hegetschweiler, K.; Micera, G.; Garribba, E. $V^{IV}O$ Versus V^{IV} Complex Formation by Tridentate (O, N_{arom} , O) Ligands: Prediction of Geometry, EPR ^{51}V Hyperfine Coupling Constants, and UV-Vis Spectra. *Inorg. Chem.* **2013**, *52*, 5260-5272.

(g) Sanna, D.; Várnagy, K.; Lihi, N.; Micera, G.; Garribba, E. Formation of New Non-oxido Vanadium(IV) Species in Aqueous Solution and in the Solid State by Tridentate (O, N, O) Ligands and Rationalization of Their EPR Behavior. *Inorg. Chem.* **2013**, *52*, 8202-8213.

(h) Kundu, S.; Mondal, D.; Bhattacharya, K.; Endo, A.; Sanna, D.; Garribba, E.; Chaudhury, M. Nonoxido Vanadium(IV) Compounds Involving Dithiocarbamate-Based Tridentate ONS Ligands:

- Synthesis, Electronic and Molecular Structure, Spectroscopic and Redox Properties. *Inorg. Chem.* **2015**, *54*, 6203-6215. (i) Dash, S. P.; Majumder, S.; Banerjee, A.; Carvalho, M. F. N. N.; Adão, P.; Costa Pessoa, J.; Brzezinski, K.; Garribba, E.; Reuter, H.; Dinda, R. Chemistry of Monomeric and Dinuclear Non-Oxido Vanadium(IV) and Oxidovanadium(V) Aroylazine Complexes: Exploring Solution Behavior. *Inorg. Chem.* **2016**, *55*, 1165-1182.
- (38) (a) Micera, G.; Garribba, E. On the prediction of ^{51}V hyperfine coupling constants in $\text{V}^{\text{IV}}\text{O}$ complexes through DFT methods. *Dalton Trans.* **2009**, 1914-1918. (b) Micera, G.; Garribba, E. Is the spin-orbit coupling important in the prediction of the ^{51}V hyperfine coupling constants of $\text{V}^{\text{IV}}\text{O}^{2+}$ species? ORCA versus Gaussian performance and biological applications. *J. Comput. Chem.* **2011**, *32*, 2822-2835. (c) Sanna, D.; Sciortino, G.; Ugone, V.; Micera, G.; Garribba, E. Nonoxido V^{IV} Complexes: Prediction of the EPR Spectrum and Electronic Structure of Simple Coordination Compounds and Amavadin. *Inorg. Chem.* **2016**, *55*, 7373-7387.
- (39) Jones, G.; Willett, P.; Glen, R. C.; Leach, A. R.; Taylor, R. Development and validation of a genetic algorithm for flexible docking1. *J. Mol. Biol.* **1997**, *267*, 727-748.
- (40) Qureshi, I. A.; Ferron, F.; Seh, C. C.; Cheung, P.; Lescar, J. Crystallographic structure of ubiquitin in complex with cadmium ions. *BMC Research Notes* **2009**, *2*, 251.
- (41) Pettersen, E. F.; Goddard, T. D.; Huang, C. C.; Couch, G. S.; Greenblatt, D. M.; Meng, E. C.; Ferrin, T. E. UCSF Chimera-A visualization system for exploratory research and analysis. *J. Comput. Chem.* **2004**, *25*, 1605-1612.
- (42) Olsson, M. H. M.; Søndergaard, C. R.; Rostkowski, M.; Jensen, J. H. PROPKA3: Consistent Treatment of Internal and Surface Residues in Empirical pK_a Predictions. *J. Chem. Theory Comput.* **2011**, *7*, 525-537.
- (43) (a) Rodríguez-Guerra, J. *Insilichem/gaudiview: Pre-alpha public releas*, Zenodo. 2017. (b) Rodríguez-Guerra Pedregal, J.; Sciortino, G.; Guasp, J.; Municoy, M.; Maréchal, J.-D. GaudiMM: A modular multi-objective platform for molecular modeling. *J. Comput. Chem.* **2017**, *38*, 2118-2126.
- (44) Connolly, M. Analytical molecular surface calculation. *J. Appl. Crystallogr.* **1983**, *16*, 548-558.
- (45) Lovell, S. C.; Word, J. M.; Richardson, J. S.; Richardson, D. C. The penultimate rotamer library. *Proteins: Struct., Funct., Bioinf.* **2000**, *40*, 389-408.
- (46) Siegbahn, P. E. M.; Himo, F. The quantum chemical cluster approach for modeling enzyme reactions. *Wiley Interdisciplinary Reviews: Computational Molecular Science* **2011**, *1*, 323-336.

- (47) Sanna, D.; Serra, M.; Micera, G.; Garribba, E. Interaction of Antidiabetic Vanadium Compounds with Hemoglobin and Red Blood Cells and Their Distribution between Plasma and Erythrocytes. *Inorg. Chem.* **2014**, *53*, 1449-1464.
- (48) Vijay-Kumar, S.; Bugg, C. E.; Cook, W. J. Structure of ubiquitin refined at 1.8 Å resolution. *J. Mol. Biol.* **1987**, *194*, 531-544.
- (49) Vilas Boas, L. F.; Costa Pessoa, J. Vanadium. In *Comprehensive Coordination Chemistry*; Wilkinson, G., Gillard, R. D., McCleverty, J. A., Ed.; Pergamon Press: Oxford, 1985; Vol. 3, pp 453-583.
- (50) Rehder, D. The potentiality of vanadium in medicinal applications. *Future Med. Chem.* **2012**, *4*, 1823-1837.
- (51) (a) Thompson, K. H.; Orvig, C. Vanadium in diabetes: 100 years from Phase 0 to Phase I. *J. Inorg. Biochem.* **2006**, *100*, 1925-1935. (b) Thompson, K. H.; Lichter, J.; LeBel, C.; Scaife, M. C.; McNeill, J. H.; Orvig, C. Vanadium treatment of type 2 diabetes: A view to the future. *J. Inorg. Biochem.* **2009**, *103*, 554-558.
- (52) Hanson, G. R.; Sun, Y.; Orvig, C. Characterization of the Potent Insulin Mimetic Agent Bis(maltolato)oxovanadium(IV) (BMOV) in Solution by EPR Spectroscopy. *Inorg. Chem.* **1996**, *35*, 6507-6512.
- (53) Sanna, D.; Buglyó, P.; Bíró, L.; Micera, G.; Garribba, E. Coordinating Properties of Pyrone and Pyridinone Derivatives, Tropolone and Catechol toward the VO²⁺ Ion: An Experimental and Computational Approach. *Eur. J. Inorg. Chem.* **2012**, *2012*, 1079-1092.
- (54) (a) Chasteen, D. N. Vanadyl(IV) EPR spin probe. Inorganic and Biochemical Aspects. In *Biological Magnetic Resonance*; Berliner, L. J. J., Reuben, J., Ed.; Plenum Press: New York, 1981; Vol. 3, pp 53-119. (b) Smith II, T. S.; LoBrutto, R.; Pecoraro, V. L. Paramagnetic spectroscopy of vanadyl complexes and its applications to biological systems. *Coord. Chem. Rev.* **2002**, *228*, 1-18. (c) Garribba, E.; Lodyga-Chruscinska, E.; Micera, G.; Panzanelli, A.; Sanna, D. Binding of oxovanadium(IV) to dipeptides containing histidine and cysteine residues. *Eur. J. Inorg. Chem.* **2005**, 1369-1382.
- (55) de Hoffmann, E.; Stroobant, V. *Mass Spectrometry Principles and Applications, Third Edition*. John Wiley & Sons Ltd.: Chichester, 2007.
- (56) Sojo, L. E.; Chahal, N.; Keller, B. O. Oxidation of catechols during positive ion electrospray mass spectrometric analysis: Evidence for in-source oxidative dimerization. *Rapid Commun. Mass Spectrom.* **2014**, *28*, 2181-2190.

- (57) Yuen, V. G.; Caravan, P.; Gelmini, L.; Glover, N.; McNeill, J. H.; Setyawati, I. A.; Zhou, Y.; Orvig, C. Glucose-lowering properties of vanadium compounds: Comparison of coordination complexes with maltol or kojic acid as ligands. *J. Inorg. Biochem.* **1997**, *68*, 109-116.
- (58) Buglyo, P.; Kiss, E.; Fabian, I.; Kiss, T.; Sanna, D.; Garribba, E.; Micera, G. Speciation and NMR relaxation studies of VO(IV) complexes with several O-donor containing ligands: oxalate, malonate, maltolate and kojate. *Inorg. Chim. Acta* **2000**, *306*, 174-183.
- (59) (a) Amin, S. S.; Cryer, K.; Zhang, B.; Dutta, S. K.; Eaton, S. S.; Anderson, O. P.; Miller, S. M.; Reul, B. A.; Brichard, S. M.; Crans, D. C. Chemistry and Insulin-Mimetic Properties of Bis(acetylacetonate)oxovanadium(IV) and Derivatives. *Inorg. Chem.* **2000**, *39*, 406-416. (b) Reul, B. A.; Amin, S. S.; Buchet, J.-P.; Ongemba, L. N.; Crans, D. C.; Brichard, S. M. Effects of vanadium complexes with organic ligands on glucose metabolism: a comparison study in diabetic rats. *Br. J. Pharmacol.* **1999**, *126*, 467-477.
- (60) (a) Liu, J.-C.; Yu, Y.; Wang, G.; Wang, K.; Yang, X.-G. Bis(acetylacetonato)-oxovanadium(IV), bis(maltolato)-oxovanadium(IV) and sodium metavanadate induce antilipolytic effects by regulating hormone-sensitive lipase and perilipin via activation of Akt. *Metallomics* **2013**, *5*, 813-820. (b) Wu, J.-X.; Hong, Y.-H.; Yang, X.-G. Bis(acetylacetonato)-oxidovanadium(IV) and sodium metavanadate inhibit cell proliferation via ROS-induced sustained MAPK/ERK activation but with elevated AKT activity in human pancreatic cancer AsPC-1 cells. *JBIC Journal of Biological Inorganic Chemistry* **2016**, *21*, 919-929.
- (61) Crans, D. C.; Khan, A. R.; Mahroof-Tahir, M.; Mondal, S.; Miller, S. M.; la Cour, A.; Anderson, O. P.; Jakusch, T.; Kiss, T. Bis(acetylamido)oxovanadium(IV) complexes: solid state and solution studies. *J. Chem. Soc., Dalton Trans.* **2001**, 3337-3345.
- (62) Garribba, E.; Micera, G.; Sanna, D. The solution structure of bis(acetylacetonato)oxovanadium(IV). *Inorg. Chim. Acta* **2006**, *359*, 4470-4476.
- (63) (a) Forbes, M. D. E.; Jarocho, L. E.; Sim, S.; Tarasov, V. F. Time-resolved Electron Paramagnetic Resonance spectroscopy. *Adv. Phys. Org. Chem.* **2013**, *47*, 1-83. (b) Neshchadin, D.; Batchelor, S. N.; Bilkis, I.; Gescheidt, G. Short-lived phenoxyl radicals formed from green-tea polyphenols and highly reactive oxygen species: An investigation by time-resolved EPR spectroscopy. *Angew. Chem., Int. Ed.* **2014**, *53*, 13288-13292.
- (64) Rangel, M.; Tamura, A.; Fukushima, C.; Sakurai, H. In vitro study of the insulin-like action of vanadyl-pyrone and -pyridinone complexes with a VO(O₄) coordination mode. *J. Biol. Inorg. Chem.* **2001**, *6*, 128-132.

- (65) Rozzo, C.; Sanna, D.; Garribba, E.; Serra, M.; Cantara, A.; Palmieri, G.; Pisano, M. Antitumoral effect of vanadium compounds in malignant melanoma cell lines. *J. Inorg. Biochem.* **2017**, *174*, 14-24.
- (66) Kiss, T.; Enyedy, É. A.; Jakusch, T. Development of the application of speciation in chemistry. *Coord. Chem. Rev.* **2017**, *352*, 401-423.
- (67) Rangel, M.; Leite, A.; João Amorim, M.; Garribba, E.; Micera, G.; Lodyga-Chruscinska, E. Spectroscopic and Potentiometric Characterization of Oxovanadium(IV) Complexes Formed by 3-Hydroxy-4-Pyridinones. Rationalization of the Influence of Basicity and Electronic Structure of the Ligand on the Properties of V^{IV}O Species in Aqueous Solution. *Inorg. Chem.* **2006**, *45*, 8086-8097.
- (68) Nguyen, B. C. Q.; Tawata, S. The Chemistry and Biological Activities of Mimosine: A Review. *Phytother. Res.* **2016**, *30*, 1230-1242.
- (69) Lodyga-Chruscinska, E.; Garribba, E.; Micera, G.; Panzanelli, A. L-Mimosine, an amino acid with maltol-type binding properties toward copper(II), oxovanadium(IV) and other metal ions. *J. Inorg. Biochem.* **1999**, *75*, 225-232.

FOR TABLE OF CONTENTS ONLY

TEXT FOR GRAPHICAL ABSTRACT. The study of the interaction of vanadium(IV) species having potential pharmacological application with ubiquitin (Ub) through spectroscopic, spectrometric and computational techniques indicates that $V^{IV}O^{2+}$ is bound to Glu16 and Glu18 residues, *cis*-octahedral VO_2 moieties (existing at mM concentrations) interact through an equatorial covalent bond with Glu16, Glu18 Asp21, or His68, while VO^+ (predominant at μM concentration) is coordinated by the sites (Glu18, Asp21) and (Glu24, Asp52).

GRAPHICAL ABSTRACT

